An-Najah National University
Faculty of Graduate Studies

Cooling of High Heat Flux Electronic Devices by Two Phase Thermosyphon System

By
Aysar Mahmoud Masoud Yasin
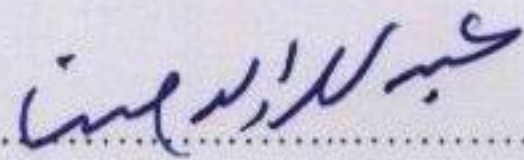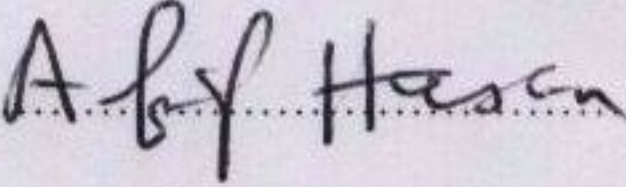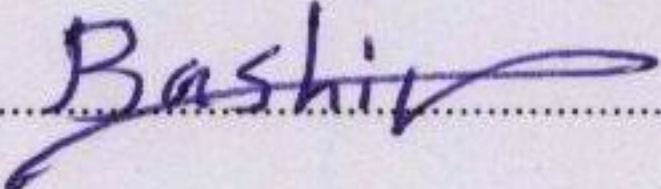
Supervisor
Dr. Abdelrahim Abusafa

Submitted in Partial Fulfillment of the Requirements for the Degree of Master of Science in Clean Energy and Energy Conservation Engineering, Faculty of Graduate Studies, An-Najah National University, Nablus – Palestine
2007

Cooling of High Heat Flux Electronic Devices by Two Phase Thermosyphon System

By
Aysar Mahmoud Masoud Yasin

This thesis was defended successfully on 2/12/2007 and approved by:

Committee Members	Signature
1. Dr. Abdelrahim Abusafa (Supervisor)	
2. Dr. Afif Hasan (External Examiner)	
3. Dr. Bashir Al Noory (Internal Examiner)	

TO My Parents

Acknowledgments

TABLE OF CONTENTS

vii

		Contents	Page No

LIST OF TABLES

LIST OF FIGURES

LIST OF SYMBOLS AND ABBREVIATIONS

A   Cross-sectional area (m²)

CHF Critical heat flux

COTS Commercial off the shelf

d   Channel inside diameter (m)

FC   Forced convection

h   Heat transfer coefficient (W/ m². ºC)

h_{fg} Latent heat of vaporization (kJ/kg)

I   Current (A)

K   Thermal conductivity (W/m ºC.)

L   Thickness (m)

$\dot{m}$ Air mass flow (kg/s)

NC   Natural convection

P   Pressure (kpa)

P_R Reduced pressure (P/Pcri)

Q   Heat load (W)

$\dot{Q}$ Rate of heat transfer (W)

q   Heat flux (W/ m²)

R   Electric resistance (Ω)

Re   Renold number

T   Temperature (°C)

T.C   Thermocouple

U   Overall heat transfer coefficient (W/ m².K)

v   Velocity (m/s)

V   Voltage difference (V)

Greek symbols

μ Dynamic viscosity (Pa.s)

ρ Density (kg/m³)

Δ Difference

σ Boltzman Constant: 5.67×10^{-8} W/m^2.K^4

ε Thermal emissivity

Subscript

amb.   Ambient

c-in   Condenser's Vapor inlet

c-out   Condenser's fluid outlet

cond.   Conduction

conv.   Convection

cri   Critical

e   Evaporator section

e-in   Evaporator's fluid inlet

e-out Evaporator's vapor (or liquid) outlet

exp   Experimental

h   Heater

rad.   Radiation

s   Surface

sat   Saturation at working pressure

surr.   Surrounding

w   Inside wall evaporator surface

Cooling of High Heat Flux Electronic Devices by Two Phase Thermosyphon System
By
Aysar Mahmoud Masoud Yasin
Supervisor
Dr. Abdelrahim Abusafa

Abstract

Two phase closed thermosyphon system for cooling high heat flux electronic devices is built in the laboratory and tested under different operating conditions.

This Study presents an experimental investigation on the heat transfer coefficient, temperature difference between the evaporator and the refrigerant inside evaporator channels, overall heat transfer coefficient, and overall thermal resistance in two-phase thermosyphon system. Investigations are carried out at different conditions: different system pressures, two different types of refrigerants R134a and R22, two different evaporator designs, natural and forced convection heat transfer mode in the condenser. The heat flux and the amount of refrigerant are the manipulated parameters in the system.

It is found that the heat transfer coefficient increases almost linearly with the applied heat to the evaporator, and reduced pressure. It is also highly dependant on the type of refrigerant, because the performance of the refrigerant R134a likely to be better than that of R22. The heat transfer coefficient is also higher at natural convection condensation than forced convection condensation at the same heat load, while the overall heat transfer coefficient in the system for forced convection is higher than for natural convection condensation. The heat transfer coefficient is highly dependant on the design of evaporator, especially on the diameters channels.

The natural convection heat transfer coefficient is found to be 27 kW/m².˚C

and 3.7 kW/m².˚C using R134a and R22, respectively at heat load of 115W. The forced convection heat transfer coefficient is found to be 2.4 kW/m².˚C and 1.6 kW/m².˚C, using R134a and R22, respectively at heat load of 450W. The forced convection overall heat transfer coefficient using R134a is found to be 9.4 kW/m².˚C at 415W while it is 1.08 kW/m².˚C at natural convection at 155W.

The temperature difference [$T_{evaporator}$–$T_{saturation}$] depends on both the applied heat flux to the evaporator, systems pressure and type of the refrigerant.

The natural convection temperature difference does not exceed 1˚C and exceeded 8˚C for R134a and R22, respectively at heat load of 100W.

The obtained evaporator temperature for R134a is 94˚C at 155W and 44˚C at 414W using natural and forced convection, respectively. While, the obtained evaporator temperature for R22 is about 80˚C at 115W and 40˚C at 450W for natural and forced convection, respectively.

The overall thermal resistance decreases almost linearly with increasing the heat load regardless of the used refrigerant. Moreover, for forced convection, the thermal resistance is much lower than the other heat transfer processes.

The overall natural convection thermal resistance is 0.47˚C/W at 155.6W and 0.53˚C/W at 115W while overall forced convection thermal resistance is 0.056˚C/W at 414W and 0.044˚C/W at 417W for R134a and R22 refrigerants, respectively.

CHAPTER ONE

INTRODUCTION

1.1 Background

Heat dissipation of electronic components is increasing to high rates that makes traditional cooling (air-cooling) ineffective method for some applications.

For example, transistors density has increased from 4 million/cm² to about 13 million/ cm². This has entailed a corresponding increase in the heat dissipated per unit area of the device. (C. Ramaswamy et al. 1999). As an example, the heat flux has increased from ~2W/cm² for Intel 486 microprocessor to about 21W/cm² for Intel P-II 300 and 400MHz microprocessors (Intel web page, 1998).

Traditional air-cooling is limited approximately to about 0.05W/cm² heat dissipation; higher heat flux rates require a very high air velocity or a significantly larger-dissipation area. To cool a component, which dissipates 100W/cm² by air-cooling, requires a heat sink about 2,000 times larger than the area of the component itself. (R. Khodabandeh and B. Palm 2002).

This level of heat flux makes the traditional cooling solution out of the thermal designer consideration, since it could not, by way or another; match the demand from these applications.

Nowadays, the thermal designer has to compute and overcome the contracting system size, insert more components within limited space, reduce the system acoustic noise generated from the heat sinks fans.

The thermal solution is required to dissipate the maximum power consumption of the electronic equipment and makes it below its maximum operating temperature.

Liquids have much higher thermal conductivities than gases, and thus much higher heat transfer coefficients associated with them. Therefore, liquid cooling is more effective than gas cooling.

There are several liquid cooling methods, one method, which is the subject of this thesis, is using a passive closed-loop two-phase thermosyphon system, which provides a promising solution to thermal challenges.

The two-phase thermosyphon passive system is a gravity dependent and wickless heat pipe. The system mainly consists of an evaporator that is attached directly to component required to cool, to make the condensate easily back to the evaporator the condenser that must be above the evaporator, the riser copper tube which is connected to the upper of the evaporator, and the down-comer copper tube which is connected to the bottom of the evaporator.

Circulation starts in the evaporator when the working fluid heats up and reach boiling conditions and the net driving head caused by the difference in density between liquid in the downcomer and vapor/liquid mixture in the riser is able to overcome the pressure drop caused by the mass flow.

The vapor bubbles starts to form at the design temperature. When the working fluid becomes vapor, its density reduces and leaves the evaporator to the condenser via the riser tube where it gets condensed and finds its way to the evaporator via the down-comer to start new circulation.

4

1.2 Objectives

1. Build up an experimental setup of an advanced two phase closed thermosyphon system as an efficient substitute to the traditional electronics air cooling,

2. Study the effect of different designs for the evaporator.

3. Investigate the effect of pressure.

4. Investigate the effect of natural and forced convection condensation.

5. Perform experiments in order to optimize the refrigerant type and dose.

6. Calculate the heat transfer, heat transfer coefficients, overall heat transfer coefficients, temperature difference [$T_{evaporator}-T_{saturation}$], and the overall thermal resistance.

7. Study the temperature distribution overall the thermosyphon system.

1.3 Motivations

1. High heat fluxes of the electronic components and limitations of heat transfer in forced-air convection have increased the need for an effective cooling to secure the lifetime of the components.

2. The desire and the general approach in electronic technology are for miniaturization of components which also has led to increased heat flux.

3. Energy conservation is becoming an important issue as the cost of fuel rises, so a closed-loop passive two phase thermosyphon system is proving a particularly effective tool in high heat flux cooling manufacture.

4. The two-phase thermosyphon system is simple to construct.

5. Compared with heat pipe, the thermosyphon system is more effective.

1.4 Methodology

The used methodology for applying this research is building up a pilot experimental setup which included evaporator, condenser, riser pipe, downcomer pipe, seven thermocouples for temperature measurements, four pressure gauges for pressure measurements, two heating elements with potentiometers and suitable insulators; make some measurements and studying the effect of important parameters such as:

1. Experimental heat transfer coefficient [h].

2. Experimental overall heat transfer coefficient [U].

3. Temperature difference [$\Delta T = T_{evaporator} - T_{saturation}$].

4. Overall Thermal resistance [R_{th}].

5. Temperature distribution in the thermosyphon system.

The above parameters are studied in accordance of the effect of changing the following factors:

- The effect of the working fluid, two different refrigerants R134a and R22 are used.

- The effect of different evaporators designs, two evaporator designs are investigated.

- The effect of different reduced pressures, four different reduced pres-

sures are used in the thermosyphon system.

- Natural and forced convection condensation are investigated.

In general, the effect of heat flux [$\dot{q}$], reduced pressure [P_R], and thermal properties of the refrigerant as well as the channel geometry on the heat transfer performance in the two-phase channel are investigated.

CHAPTER TWO

LITERATURE REVIEW

Two phase closed thermosyphon cooling technique is considered as one of the strongest alternative cooling technologies that is being tested and re-searched by specialized researchers and students in the field of electronics cooling. It has become important due to the limit capacity of conduction, natural and forced-air cooling on high heat flux elimination.

Several studies and researches are carried out in this subject to improve the efficiency and reliability of the high heat flux thermosyphon system. This chapter, deals with heat transfer calculation, behavior, characteristics, analysis, and thermal performance and a brief description of some studies is illustrated.

R. Khodabandeh, (2005) investigated experimentally the Pressure drop in riser and evaporator in an advanced two-phase thermosyphon loop and he found that the total pressure drop in the riser is the sum of the gravitational and frictional pressure drop.

R. Khodabandeh, (2004) studied Heat transfer in the evaporator of an ad-vanced two-phase thermosyphon loop and he found that heat transfer is weakly dependent on vapor fraction but highly dependent on heat flux and system pressure, indicating that nucleate boiling is the dominant mechanism and for different diameters of evaporator channels the heat transfer coeffi-cient slightly increases with increasing vapor fraction.

Palm and Khodabandeh, (2003) studied the parameters taken into account for choosing working fluid for two-phase thermosyphon systems for cooling of electronics and they found that increased pressure level generally leads to lower temperature difference and smaller tubing diameter. It has been stated that there are no ideal working fluids.

R. Khodabandeh, (2003) investigated the thermal performance of a closed advanced two-phase thermosyphon loop for cooling a radio base stations at different operating conditions and he found that the thermal resistance between the heat source and the evaporator is the highest thermal resistance for both forced and free convection, natural convection gives a higher thermal resistance than forced convection, the heat transfer coefficient in the evaporator channels is higher for natural convection at heat fluxes larger than 100 kW/m² due to higher system pressure at these ranges, and finally he concluded that the thermal resistances between the heat source/evaporator and the condenser/air are dominating in the thermosyphon system compared with resistances between the evaporator walls and the condenser walls.

K.S. Ong and Md Haider-E-Alahi (2002) studied the thermal performance of a thermosyphon filled with R-134a, they found that the performance of the R-134a thermosyphon increased with high coolant mass flow rates, high fill ratios and greater temperature difference between bath and condenser.

Khodabandeh and Palm, (2002) studied the Influence of system pressure on the boiling heat transfer coefficient in a closed two-phase thermosyphon loop and they concluded that pressure has a significant effect on the boiling heat transfer coefficient in the narrow channels of the thermosyphon evaporator and also the heat transfer coefficient at most points at a given heat flux is more than three times larger at the reduced pressure $P_R = 0.3$ than $P_R = 0.02$. Comparing smooth and threaded channels, using Isobutane as a refrigerant, the heat transfer coefficient at all pressures were considerably improved by the threads.

Khodabandeh and Palm, (2002) studied an experimental investigation of

critical heat flux (CHF) in a vertical narrow channel in an advanced thermosyphon loop and they found that the threaded surface has a minor effect on CHF.

Pioro et al, (2001) studied the influence of pressure on CHF, and found that limit critical quality decreases with an increase in pressure, but increases with increase in diameter.

The pressure level in the system has a significant effect on the CHF. The CHF can be improved by using the higher pressure in the system. As mass flow increases and a large number of cavities activated by increasing the pressure in an advanced loop two-phase thermosyphon, the CHF will be improved. (R. Khodabandeh and B. Palm 2001)

R. Khodabandeh and B. Palm, (2001) investigated the influence of the threaded surface on the boiling heat transfer coefficients in vertical narrow channels, they found that achieving a low temperature difference and high heat transfer coefficient in the thermosyphon system using a threaded surface in the evaporator section with R134a and R600a as refrigerants. It was found that with the threaded surface the temperature difference in the evaporator decreased to about half for R134a and even more for R600a. The largest enhancements were found at the highest heat fluxes. Because heat transfer coefficient was dependent on heat flux, the dominant boiling mechanism was thought to be nucleate boiling.

Rhi and Lee, (1999) found that a cooling heat flux of 12 W/cm² and 5 W/cm² at an overall temperature difference of 50˚C could be achieved under forced and free convection respectively. The result was obtained during study of an advanced two-phase flow thermosyphon loop for cooling of electronic

components using acetone or FC87 as working liquid.

C. Ramaswamy et al, (1999) investigated the thermal performance of a compact two-phase thermosyphon: response to evaporator confinement and transient loads and shows that high heat transfer rates (up to $100W/cm^2$). The enhanced structure used demonstrates almost 2.5 times increase in the heat transfer compared to a solid block of the same size.

Kasza et al, (1997) found that in large cross-section channels, a much higher wall superheat and longer channels are needed to have enough vapor to form large vapor slugs that occupy the entire channel. They suggested the mentioned phenomenon as one possible reason of higher heat transfer coefficient and much broader nucleate boiling conditions for narrow channels compared to the large sized channels.

Lin et al, (1997) showed that at low vapor quality, the heat transfer is mainly heat flux dependent, indicating nucleate boiling, while at higher quality heat transfer is independent of heat flux but dependent on quality and mass flux, indicating dominance of convective boiling.

McDonald et al, (1997) studied thermosyphon loop performance characteristics and they found that for a given loop orientation and charge the performance will be affected by changes in the source and sink temperatures. For a given source, sink temperature difference the performance was found to be improved with increasing loop pressure.

Webb et al, (1996) used enhanced surfaces in the evaporator and condenser sections of a thermosyphon for cooling the hot side of thermoelectric coolers. Using a "bent-fin" structure, they have achieved a heat flux of about

$18W/cm^2$ in refrigerant R-134a. Performance evaluation was carried out over a range of velocities for the forced convection cooled condenser.

The effect of pressure on the boiling heat transfer coefficient have been studied by many researchers such as Cooper, (1984) and Gorenflo, (1987) and all agreed on that the boiling heat transfer coefficient increases with increasing pressure.

CHAPTER THREE

THEORETICAL BACKGROUND

3.1 Introduction

Cooling is preferable to be named by others as thermal control is a critical engineering science that must be accurately implemented to ensure the required performance and reliability.

Electronic components depend on the passage of electric current to perform their duties, and they become potential sites for excessive heating. The race towards miniaturization of electronic devices such as laptops increases dramatically the heat generated per unit volume.

Electronic parts fail catastrophically from simple overheating, so the prevention of thermal failure must be the primary goal of all thermal management schemes.

Several methods are used for this purpose; this chapter introduces several cooling techniques that are commonly used in electronic equipment such as: conduction cooling, radiation and natural air convection, forced air convection, immersion cooling, jet impingement cooling, spray cooling, and heat pipe cooling.

The criteria of choosing the appropriate cooling method for electronic equipment depends on many factors; the magnitude of heat generated, reliability requirements, environmental conditions and cost.

Natural or forced convection is used for low-cost electronic equipment while more complicated cooling techniques are adopted for high-cost cooling.

3.2 Cooling Heat Transfer Modes

Cooling processes, saying nothing that their configurations depend on its operation on one of the three distinct heat transfer modes: conduction, convection and radiation.

3.2.1 Conduction Heat Transfer

It is the transfer of energy from the more energetic particles of a substance to the adjacent less energetic ones as a result of interactions between the particles.

The one-dimensional steady heat transfer conduction through a plane is given by a relation called the **Fourier's law of conduction** :

$$\dot{\mathbf{Q}} = \mathbf{k} \times \mathbf{A} \, \frac{\mathbf{\Delta T}}{\mathbf{L}} \tag{3.1}$$

Where k is the thermal conductivity, L is the plane thickness, A is the surface area, and ΔT is the temperature difference.

3.2.2 Convection Heat Transfer

It is the mode of energy transfer between a solid surface and the adjacent liquid or gas is in motion, and it involves the combined effects of conduction and fluid motion.

The convection heat transfer from a surface at Temperature T_s to a fluid at temperature T_{fluid} is given by a relation called Newton's Law of Cooling:

$$\dot{\mathbf{Q}}_{\mathbf{conv}} = \mathbf{h}_{\mathbf{conv}} \times \mathbf{A} \times \mathbf{\Delta T} = \mathbf{h}_{\mathbf{conv}} \times \mathbf{A} \times (\mathbf{T_s} - \mathbf{T_{fluid}}) \tag{3.2}$$

Where h_{conv} is the convection heat transfer coefficient $W/m^2.°C$.

3.2.3 Radiation Heat Transfer

It is the energy emitted by matter in the form of electromagnetic waves (or photons) as a result of the changes in the electronic configurations of the atomic and molecules. Unlike conduction and convection, the transfer of energy by radiation does not require the presence of an intervening medium.

Radiation heat transfer between a surface at temperature T_s surrounded by a much larger surface at temperature T_{surr} can be expressed as:

$$\dot{Q}_{rad} = \varepsilon \times A \times \sigma \times (T_s^4 - T_{surr}^4) \tag{3.3}$$

Where σ is Boltzman constant = 5.67×10^{-8} W/m^2.K^4, and ε is the thermal emissivity.

Radiation depends on temperature of radiating surfaces, temperature of surroundings, surface conditions, shielding effects of neighboring surfaces.

3.3 Calculation of Cooling Load of Electronic Equipment

Determination of heat dissipation (cooling load) from electronic equipment is the first step in the selection and design of a cooling system.

Measuring the applied voltage (V) and electric current (I) at the input of the electronic device under full load conditions. The electric power which is the heat dissipation could be found from the following relation with exception to the equipment that outputs other forms of energy such as emitter tubes of radar.

$$\dot{Q} = \dot{W}_e = V \times I = I^2 \times R \tag{3.4}$$

3.4 Cooling Techniques

This section illustrates and defines the most important and applied methods of both air and liquid electronic cooling techniques.

1.3.4.1 Conduction Cooling

It is based on the diffusion of heat through a solid, liquid, or gas as result of molecular interaction in the absence of any bulk motion.

The advantages of conduction cooling : the installation structures may be utilized to reach an ultimate "heat sink" such as the ambient environment or a large system/platform heat exchanger, module cards may use attached thermal planes of aluminum, copper or other material to transfer heat from components to other locations such as conduction/convection heat exchangers, basic conduction mechanisms require no extra pumps, ducting, filters, collection reservoirs, etc, and finally it may be inexpensive unless more expensive materials are used. (Systems design and analysis, 2000)

Conduction cooling disadvantages:

1. It requires high pressure, intimate contact between heat transfer surfaces.

2. Material thermal conductivity dependant.

3. Thermal paths through multiple parts and surfaces will impose thermal resistances.

4. Transfer surfaces must be maintained free of corrosion.

5. Transfer surfaces must be free from vibration-induced failures.

3.4.2 Radiation and Natural Air Convection.

Low-power electronic systems are conveniently cooled by natural convection and radiation. Natural convection cooling is very desirable since it does not involve any fans that may break down.

Natural cooling is effective when the path of the fluid is relatively free of obstacles and is less effective when the fluid has to pass through narrow flow passages and over many obstacles. Natural convection is based on fluid motion caused by the density differences in a fluid due to a temperature difference.

The natural heat transfer rate is directly related to the flow rate of the fluid, it also depends on the temperature difference between the fluid adjacent to a hot surface and the fluid a way from it.

Thermal radiation is defined as energy emitted by matter at a finite temperature where the energy of the radiation field is transported by electromagnetic waves. (Incropera and DeWitt, 2002)

The magnitude of radiation heat transfer, in general, is comparable to the magnitude of natural convection heat transfer. This is specially the case for surfaces whose emissivity is close to unity.

Circuit boards that dissipate up to about 5W of power or that have power density of about 0.02 W/cm² can be cooled effectively by natural convection.

Natural Convection and radiation cooling can be improved by attaching fins to the surfaces; Figure 3.1 shows extended surfaces used for this purpose.
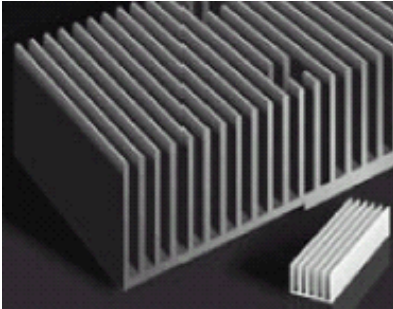
Figure 3.1: Extended surface to enhance convective and radiative heat transfer.

3.4.3 Forced Air Convection

Forced convection occurs when flow over a cooled surface is caused by external means such as a fan, a pump, a jet of air, or atmospheric winds.

Convection heat transfer between a solid surface and a fluid is proportional to the velocity of the fluid, large flow rate comes higher heat transfer rate.

When natural convection cooling is not adequate, a forced convection is resorted in order to enhance the velocity and thus increasing the heat transfer coefficient by factor up to 10 depending on the size of the fan. This means the surface temperature of the components can be reduced considerably for specified power dissipation. The radiation heat transfer in forced convection cooled electronic systems is usually disregarded.

Forced convection cooling is more complicated than natural convection cooling, but has the ability of maintaining higher heat extraction rates. Forced convection cooling has the same dependencies as natural convection but in addition, is greatly influenced by fluid velocity and the type of flow pattern present within the cooling medium. Higher heat transfer rates can be reached with turbulent flow where chaotic flow patterns are dominant.

The choice of cooling medium is very important. Forced air convection has the following advantages above that of forced liquid cooling:

1. The supply of cooling air is readily available.

2. Does not have freezing, boiling and dripping problems.

Some drawbacks to the use of forced air-cooling are not suitable at high altitude or low air density locations, acoustic noise, vibrations, and the ejection of hot air could negatively affect the surroundings.

3.4.4 Liquid Cooling

Liquids have much higher thermal conductivities than gases and thus much higher heat transfer coefficients associated with them. Therefore, liquid cooling is far more effective than gas cooling which makes it reserved for applications involving power densities that are too high for safe dissipation by air-cooling.

Liquid cooling system where heat generated in the components is transferred directly to the liquid is called direct cooling and the system where the heat generated is first transferred to a medium such as a cold plate before it carried away by the liquid is called indirect cooling system.

The liquid cooling systems whether direct or indirect are classified as open loop and closed loop; in the open loop, such as open loop immersion cooling system, the liquid is drained after it is heated while the in the closed system, such as heat pipe, the liquid is re-circulated through the system.

Direct and indirect liquid cooling methods can each be further categorized into single-phase and two-phase liquid cooling. Two-phase cooling methods

are more desirable because of high heat transfer coefficients.

Two-phase flows are commonly found in industrial processes and in ordinary life. Gas-liquid flow occurs in boiling and condensation operations, liquid-liquid flow occurs in liquid-liquid extraction process, gas-solid flow occurs in fluidized bed, and solid-liquid flow occurs during the flow of suspensions such as riverbed sediments. (Whalley, 1996)

There are several different liquid cooling technologies such as immersion cooling, heat pipe cooling, jet impingement cooling, spray cooling and thermosyphon cooling.

3.4.4.1 The Immersion Cooling.

In direct cooling, electronics are immersed into a dielectric liquid. The closed loop systems are normally used due to both: liquids cost and environmental issues associated with the liquids leakage into the atmosphere.

The simplest type of immersion cooling system involves an external reservoir, which supplies liquid continually to the electronic enclosure. The generated vapor is allowed to escape to atmosphere. A Pressure relief valve on the vapor vent controls the inside pressure and the temperature inside at the preset values. (Çengel, 2003)

Figure 3.2 shows closed loop immersion cooling system with external condenser, the electronics expel heat into the liquid where vapor bubbles are formed, vapor is collected at the top of the enclosure where it comes in contact with some sort of heat exchanger. The vapor condenses and returns to the liquid portion of the reservoir.
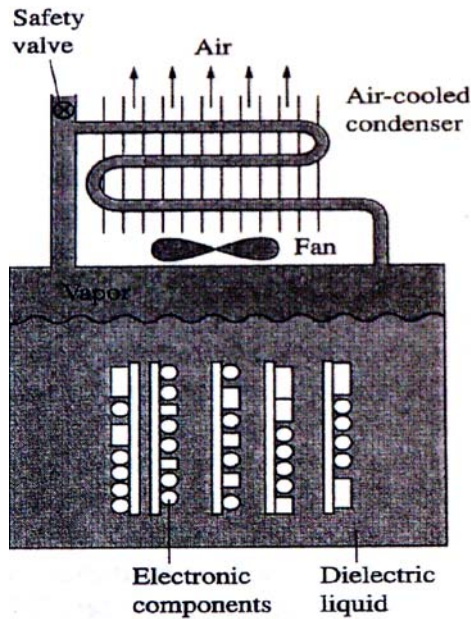
Figure 3.2: Closed loop immersion cooling system with external condenser. (Çengel, 2003)

Figure 3.3 shows the typical ranges of the heat transfer coefficients for various dielectric fluids suitable for use in cooling of electronic equipment.

Immersion Cooling System Disadvantage:

1. Leakage concerns which causes low reliability and environmental hazards.

2. The introduction on incompressible gases into the vapor space limits the amount of condensation, which consequently degrade heat transfer. (Çengel, 2003)

3. The fluid used for immersion boiling has to be chemically compatible with the components and must have a large dielectric strength. This limits the choice of fluids. (Palm, R. Khodabandeh 2003)
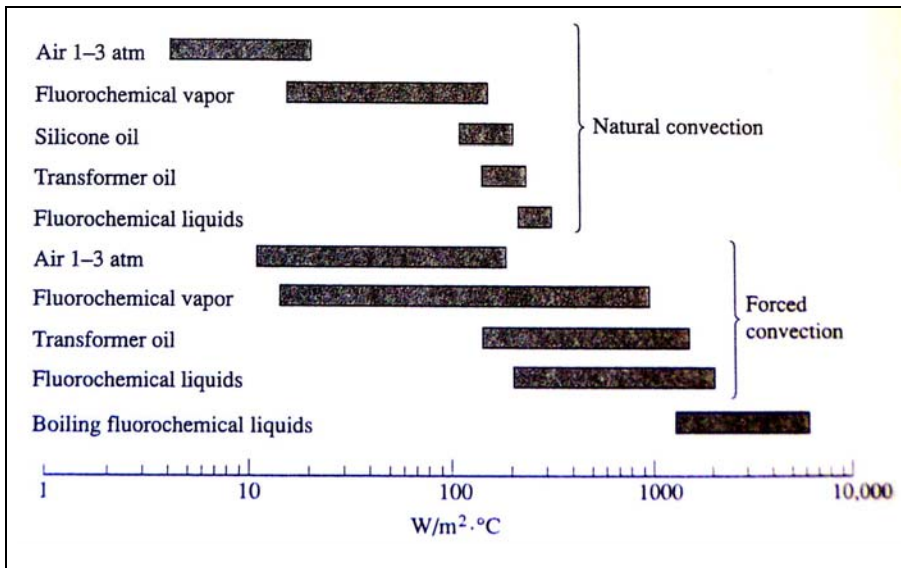
Figure 3.3: Typical heat transfer coefficients for various dielectric fluids. **(**Çengel, 2003)

3.4.4.2 Jet Impingement

Jet impingement is a technique for enhancing heat transfer that is employed in a variety of applications ranging from drying of textiles and films, to metal sheet manufacturing and to gas turbine and electronic equipment cooling.

Jet impingement is an attractive cooling mechanism due to the capability of achieving high heat transfer rates. This cooling method has been used in a
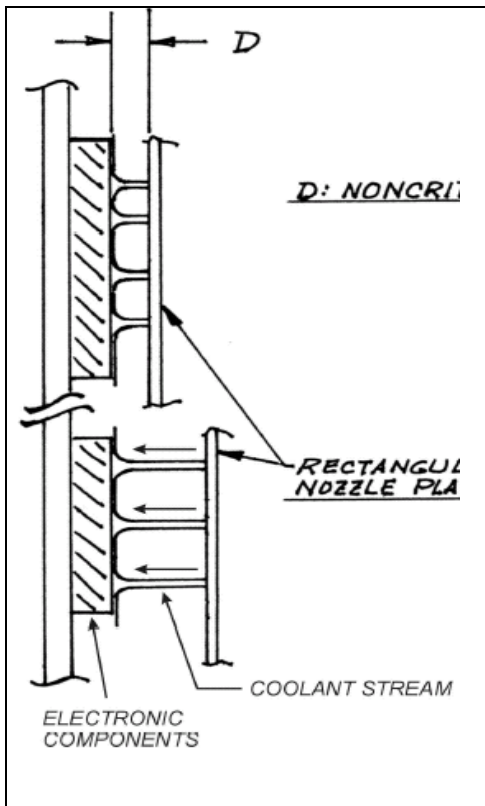
Figure 3.4: Jet impingement cooling configuration. (Systems design and analysis, 2000)

wide range of industrial applications such as annealing of metals, cooling of gas turbine blades, cooling in grinding processes. (Babic et al, 2005)

Jet impingement has also become a viable candidate for high-powered electronic and photonic thermal management solutions and numerous jet impingement studies have been aimed directly at electronics cooling. (Narumanchi et al, 2003)

A fluid jet issuing into a region containing the same fluid is characterized as a submerged jet while a fluid jet issuing into a different, less dense, fluid is characterized as a free-surface jet.

Womac et al, (1990) have shown that higher heat transfer coefficients result from submerged jet conditions than from free-surface jet conditions for $Re \geq 4000$.

An impinging jet is said to be confined or semi confined if the radial spread is confined in a narrow channel, usually between the impingement surface and the orifice plate.

The advantages of jet impingement are summarized as following: very high heat fluxes can be achieved if desired, critically designed/manufactured nozzles not required, plates with machined openings can be used, flow can be localized if only a single jet is used, multiple jets placement is not as critical with respect to closeness to/from parts, Jet hardware is more repeatable and durable due to less precision required in jet openings, will not splash and separate away from parts, there is no cone effect requiring specific locations with respect to parts, thermal transfer can also take place in sensible regime better than with spray.(Systems design and analysis, 2000)

Disadvantages:

1. The concentration of heat removal within the impingement zone may cause large temperature gradients within the cooled devices. (Mudawar, 2000)

2. During vigorous boiling, there is a risk of separation of the liquid layer from the impingement zone. (Mudawar, 2000)

3. Requires complex fluid handling and reconditioning (condensation, heat exchange with ultimate "sink," etc) hardware. This adds weight and associated penalties to platform systems. (Systems design and analysis, 2000)

3.4.4.3 Spray Cooling

A simplified drawing of the Spray Cooling concept is shown in Figure 3.5.
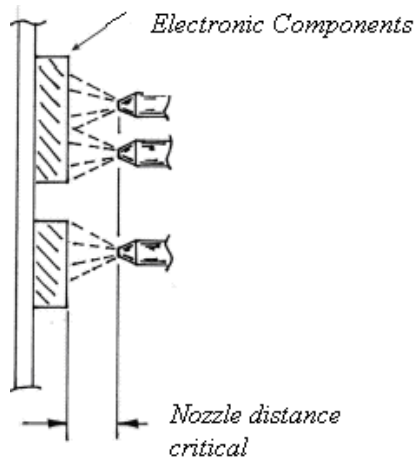
Figure 3.5: Spray cooling configuration example. (Systems design and analysis, 2000)

Spray Cooling offers good performance in applications with low to moderate heat removal requirements.

The individual Spray Cooling components, such as nozzles, plumbing, pumps, filters, and heat exchangers are commercially producible.

Advantages:

1. Can provide high heat flux.

2. Gives good coverage due to atomizing action

3. May use less fluid than forced convection, bulk flow mechanism

4. May use slightly less fluid than jet impingement. (System design and analysis, 2000)

Disadvantages:

1. The complicated flow feature with spray nozzles, and the possibility of clogging of the nozzles.

2. They need careful and periodic testing for nozzles and higher temperature difference compared to nucleate boiling. (Mudawar, 2000)

3. Requires special spray nozzles.

4. Requires complex fluid handling and reconditioning (condensation, heat exchanger with ultimate "sink", etc) equipment. This adds weight and associated penalties to platform systems.

5. Quality control is critical. Nozzles are very sensitive to manufacturing tolerances and quality.

6. Nozzle action can change in time due to erosion, corrosion build up, and contaminants.

7. Spray velocity and momentum can be critical. If too great, it can lead to part erosion, and splashing away without proper wetting of the part surfaces, leading to poor cooling.

8. Proper distance and some degree of confinement has been found necessary to avoid separation from surfaces, leading to poor wettability.

9. Has poor sensible cooling action. (Systems design and analysis, 2000)

3.4.4.4 Heat Pipe Cooling Technology

It is a simple device with no moving parts that can transfer large quantities of

heat over fairly large distances essentially at constant temperature without requiring any power input.

A heat pipe is basically a sealed slender tube containing a wick structure lined on the inner surface and small amount of fluid at a saturated state, Figure 3.6 shows the basic components.

It is composed of three sections: the evaporator section at one end, where heat is absorbed and the fluid is vaporized. A condenser section at the other end, where the vapor is condensed and heat is rejected. And the adiabatic section on between, where the vapor and the liquid phases of the fluid flow in opposite direction through the core and the wick, respectively.

Wick structures on the inner walls of the heat pipe provide capillary forces to pump the condensate back to the hot end of the heat pipe completing the continuous evaporation/condensation cycle.
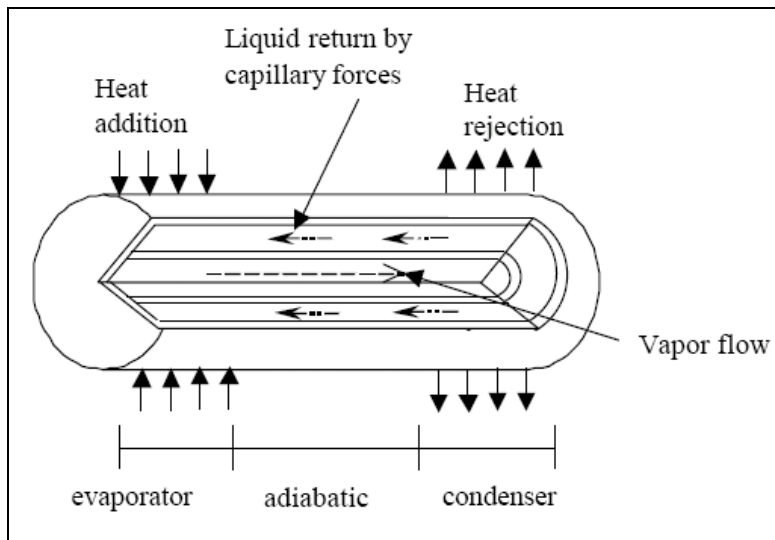
Figure 3.6: Structure and principle of heat pipe. (Ali, 2004)

The main application of the heat pipes is on electronics cooling where small high performance components cause high heat fluxes and high heat dissipation demands. It is used to cool transistors and high-density semiconductors. Other fields of applications are aerospace and heat exchangers.

Advantages:

1. Simple structure, lightweight, no mechanical components, and no power consumption. (Ali, 2004)

2. Very high thermal conductivity. less temperature difference needed to transport heat than traditional materials (thermal conductivity up to 90 times greater than copper for the same size) (Faghiri, 1995) resulting, in low thermal resistance. (Peterson, 1994)

3. Power flattening, A constant condenser heat flux can be maintained while the evaporator experiences variable heat fluxes. (Faghiri, 1995)

4. Efficient transport of concentrated heat. (Faghiri, 1995)

5. Temperature Control, The evaporator and condenser temperature can remain nearly constant (at T_{sat}) while heat flux into the evaporator may vary (Faghiri, 1995)

6. Geometry control. The condenser and evaporator can have different areas to fit variable area spaces (Faghiri, 1995). High heat flux inputs can be dissipated with low heat flux outputs only using natural or forced convection. (Peterson, 1994)

Main Types of Heat Pipes:

1. Thermosyphon heat pipe: gravity assisted wickless heat pipe. Gravity is used to force the condensate back into the evaporator. Therefore, condenser must be above the evaporator in a gravity field.

2. Leading edge heat pipe: placed in the leading edge of hypersonic vehicles to cool high heat fluxes near the wing leading edge. (Faghiri, 1995)

3. Rotating and revolving heat pipe: condensate returned to the evaporator through centrifugal force. No capillary wicks required. Used to cool turbine components and armatures for electric motors.

4. Cryogenic heat pipe: low temperature heat pipe. Used to cool optical instruments in space. (Peterson, 1994)

5. Flat Plate heat pipe: much like traditional cylindrical heat pipes but are rectangular. Used to cool and flatten temperatures of semiconductor or transistor packages assembled in arrays on the top of the heat pipe. (Faghiri, 1995)

6. Micro heat pipes: small heat pipes that are noncircular and use angled corners as liquid arteries. (Peterson, 1994)

7. Variable conductance heat pipe: allows variable heat fluxes into the evaporator while evaporator temperature remains constant by pushing a non-condensable gas into the condenser when heat fluxes are low and moving the gas out of the condenser when heat fluxes are high, thereby, increasing condenser surface area. They come in various forms like excess-liquid or gas-loaded form. Used in electronics cooling. (Faghiri, 1995)

8. Capillary pumped loop heat pipe- for systems where the heat fluxes are very high or where the heat from the heat source needs to be moved far away. In the loop heat pipe, the vapor travels around in a loop where it condenses and returns to the evaporator. Used in electronics cooling. (Faghiri, 1995)

3.5 Comparison between Cooling Techniques

Figure 3.7 compares between the commercial off the shelf (COTS) electronics cooling techniques from the following point of views:

- Complexity,

- Weight,

- Cost,

- Cooling capacity,

- Overall ratings.
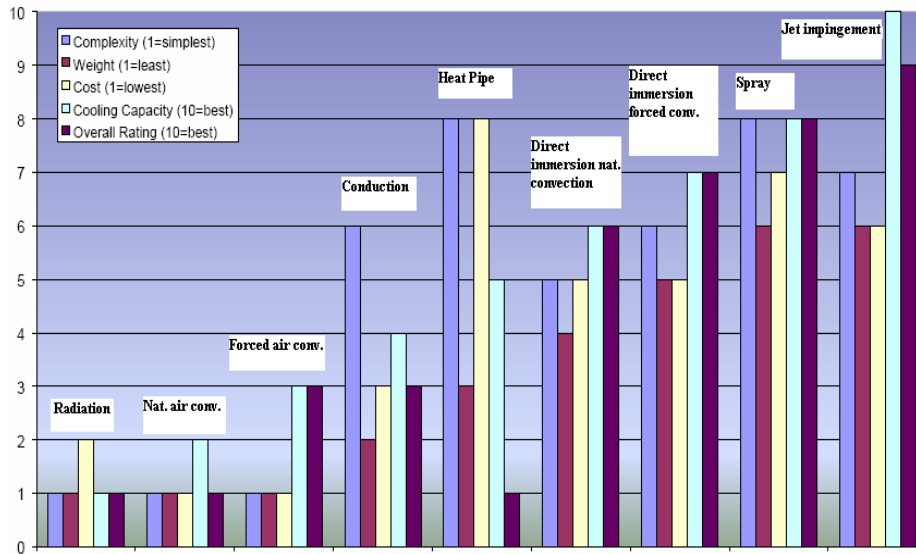
Figure 3.7: Comparison between Commercial off the shelf (COTS) electronics cooling techniques. (Systems design and analysis, 2000)

3.6 Important Parameters for Selecting Refrigerant

Reliability, Compactness, inexpensiveness, good cooling and safety are the general goal of the design of any cooling system. Higher pressure fluids will give better performance and more compact designs (Palm, R. Khodabandeh, 1999).

1. Pressure Drop

The pressure drop in the cycle depends not only on the volume flow rate, but also on the density and viscosity of the fluid.

Palm and Khodabandeh (1999) stated that the pressure drop decreased with increasing saturation pressure. For a certain tube length, diameter and cooling capacity. the pressure drop is a function of the viscosity, density and heat of vaporization.

$$\Delta P = 0.241L \ \frac{\dot{Q}^{7/4}}{d^{19/4}} \ Dp \qquad\qquad (3.5)$$

Where L is thickness (m), d is Channel inside diameter (m), $\dot{Q}$ is rate of heat transfer (W), and Dp is called figure of merit.

$$Dp = \frac{\mu^{1/4}}{\rho \cdot h_{fg}^{7/4}} \qquad\qquad (3.6)$$

Where h_{fg} is Latent heat of vaporization (kJ/kg), and ρ is density (kg/m³), and μ is dynamic viscosity (Pa.s)

This ratio (Dp) is plotted versus saturation pressure in Figure 3.8.
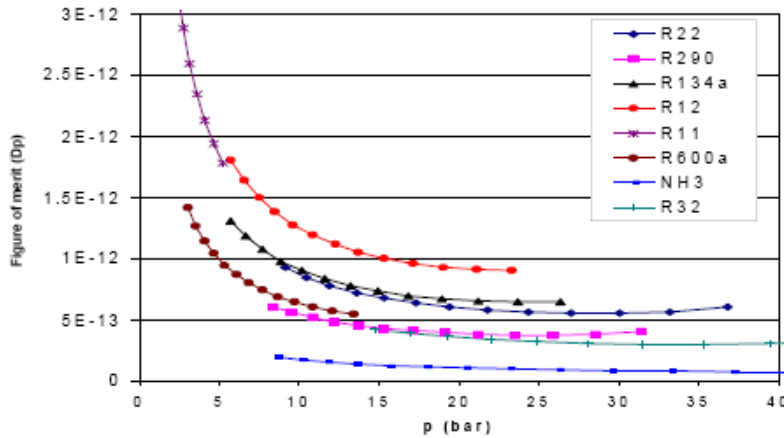
Figure 3.8: Figure of merit for one-phase vapor flow pressure drop as a function of saturation pressure. (Palm, R. Khodabandeh, 2000)

2. Evaporation and Condensation

The boiling heat transfer influenced by pressure level, this fact is illustrated in Figure 3.9, which is a draw to the boiling heat transfer coefficients versus reduced pressure for two fluids with different molecular weight according to

(Cooper, 1984) and (Gorenflo, 1993)

From Figure 3.9, it is clear that the heat transfer coefficients can be expected to increase with increasing reduced pressure and with decreasing molecular weight.

In condensation, heat transfer may be governed by conduction through a laminar free-falling film as described by (Nusselt, 1916)
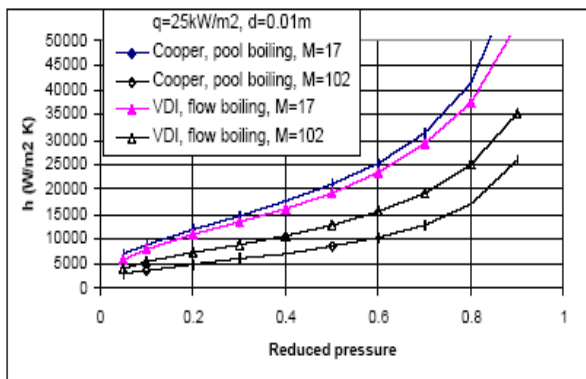
Figure 3.9: Boiling heat transfer coefficients according to cooper (1984) and Geornflo (1993) vs. reduced pressure for two fluids with different molecular weight.

3. Critical Heat Flux

Critical heat flux (CHF) is considered as one of the most important parameters in selecting working fluid.

Lienhard and Dhir (1973a, b) found a correlation between the saturation temperature and the critical heat flux for different types of workings fluids. Ammonia (NH$_3$) has shown outstanding critical heat flux 5 times higher than the other fluids because of its extremely high heat of vaporization as shown in Figure 3.10. R-32 has maximum critical heat flux after ammonia

while the R-11 has the minimum.
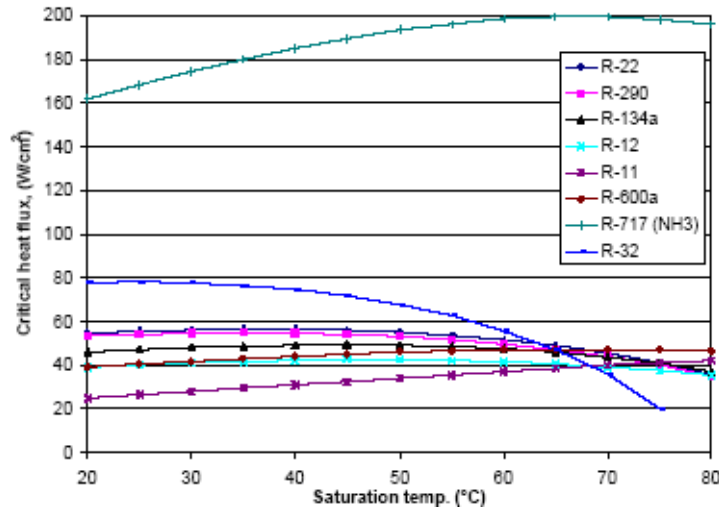
Figure 3.10: Critical heat flux of different fluids according to Lienhard and Dhir correlation (1973 a, b)

4. Environment, Price and safety Requirements

There are several other requirements which should be met: (Palm and Khodabandeh 2000)

1. The fluid should not be harmful to people during production, normal operation or in case of a breakdown.

2. It should not be harmful to the equipment in which it is installed. This means that it should not be explosive or flammable, not corrosive or otherwise incompatible with the materials of the equipment.

3. It should not be harmful to the global environment. This means that it should have a zero ozone depletion potential (ODP), it should not contribute to the greenhouse effect, not be hazardous to animals or plants or have de-

composition products which have such effects. Preferably, it should be a naturally occurring substance to eliminate the risk of unknown environmental effects.

4. From an operational point of view, the fluid should be able to withstand the environment of the equipment for a long period of time without decomposing.

5. Finally, it should have a low price and be readily available.

CHAPTER FOUR

EXPERIMENTAL SETUP AND PROCEDURES

4.1 Set-up Design

The schematic diagram of the tested thermosyphon system setup is shown in Figure 4.1.
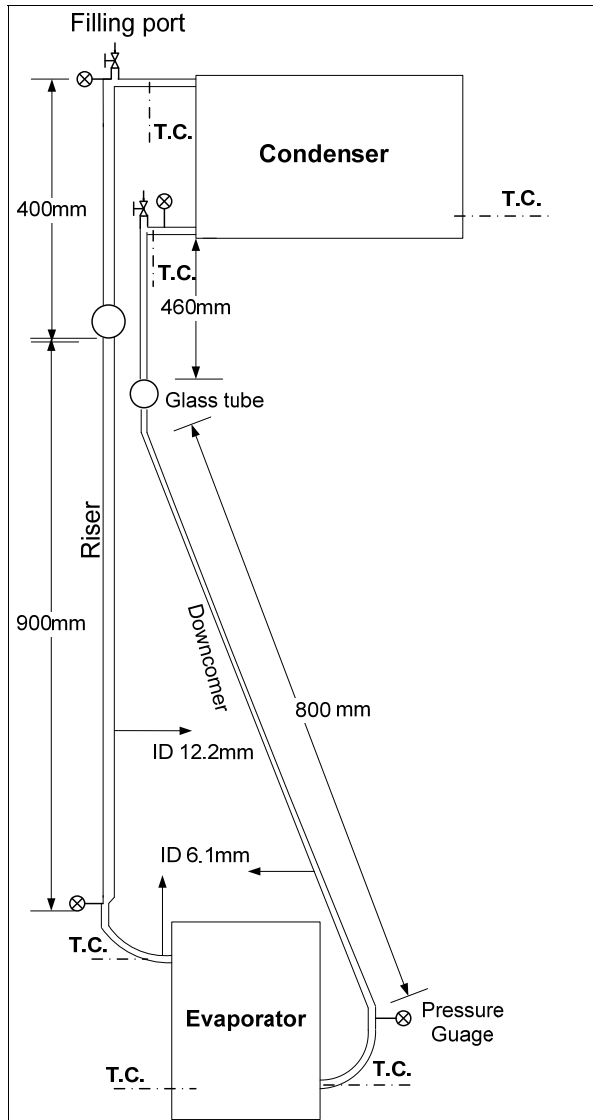
Figure 4.1: Schematic diagram of the tested thermosyphon system

The two-phase thermosyphon system set-up is built to verify the performance hypotheses and demonstrate the effectiveness of the system as a passive cooling system solution for high heat flux electronic devices.

The set-up consists of the following components:

1. **Evaporator**

Two different designs of evaporators are investigated. The tested evaporators are made from copper, the outer dimension of both evaporators are 63×50×20 as shown in Figure 4.2. The weight of each evaporator is nearly the same, which is about 440 gram.
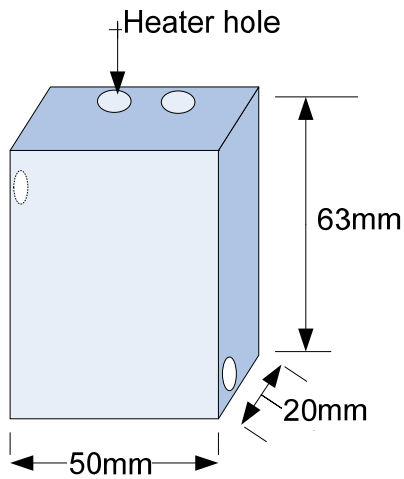
Figure 4.2: External shape of the evaporators.

The internal design of channels and the top view of the first tested evaporator are illustrated in Figures 4.3 and 4.4, respectively. Throughout this thesis, the evaporator shown in Figure 4.3 will be designated as **_evaporator-1_**.

R =2.5mm

37mm

40mm

6mm
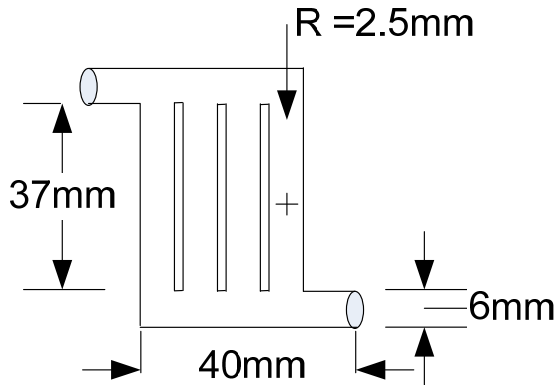
Figure 4.3: Internal channels of the tested evaporator-1

The dimensions of the internal channels of evaporator-1 are illustrated in Figure 4.3, four vertical channels with diameter of 5 mm, length of 37 mm, and total internal surface area of 34.5 cm².

R=2.5mm
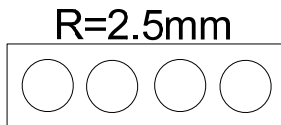
Figure 4.4: Top view of the tested evaporator-1

The internal design of channels and top view of the second tested evapo-rator are illustrated in Figures 4.5 and 4.6, respectively. Throughout this thesis, the evaporator shown in Figure 4.5 will be designated as *evaporator-2*.
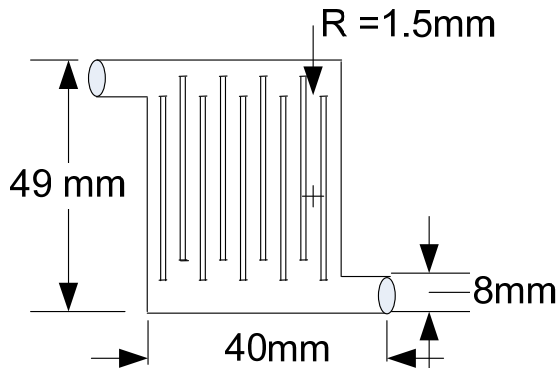
Figure 4.5: Internal channels of the tested evaporator-2

The dimensions of the internal channels of evaporator-2 is illustrated in Figure 4.5, Ten vertical channels with diameter of 3 mm, length of 37 mm, and total internal surface area of 50 cm².
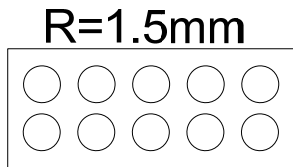
Figure 4.6: Top view of the tested evaporator-2

The heat transfer from the evaporator to the downcomer and riser is eliminated by putting a short piece of rubber hose in between.

Two cartridge heaters are used in the experiment, each of 250W capacity, and they are exactly inserted into two cylindrical holes drilled in the evaporator. In order to reduce the contact resistance as much as possible between the heaters and the evaporator surfaces, special epoxy material is filled in between. The diameter of each heater is 6.2mm with 50mm depth with surface area of 9.73 cm². Figure 4.7 illustrates the cartridge heater used
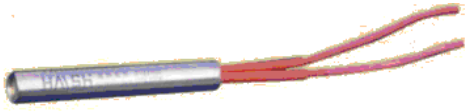
in the experiments.

Figure 4.7: The cartridge heater used in the experiment

The power of the heaters is equally distributed to the evaporator channels and is varied in steps from (4–150) W at natural convection condensation and from (8–450) W at forced convection condensation. For this purpose, the heaters are connected to a potentiometer with solid-state relay.

Figure 4.8 shows the position of the evaporator's internal channels with respect to heaters holes and shows the direction of refrigerant flow in the system.
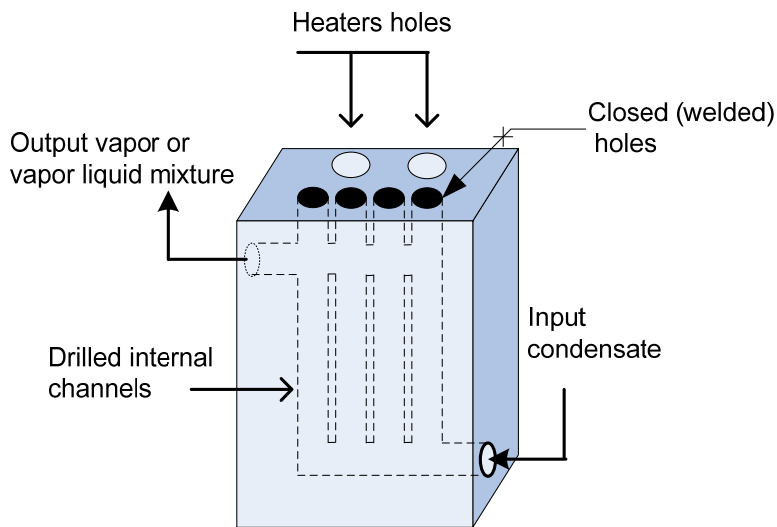
Figure 4.8: Position of evaporator's internal channels with respect to heaters holes

The heat supplied from the heaters is assumed to be dissipated through the

evaporator without considerable losses because of the well-done insertion of the heaters through the evaporator as well as the tight insulation of the evaporator it self using 3mm rock wool thickness insulation.

2. Condenser

An aluminum-finned condenser with the fins oriented vertically that can be cooled by free or forced convection is used. It consists of 120 parallel plates Each plate dimension is 4.4 × 25 cm² with inter plate distance of 3mm. The total outer surface area of the plates is 1.32 m² at the airside.

3. Riser and downcomer

Both the downcomer and riser is constructed from Copper tubing which is known of its high corrosive resistivity against most HFCs

The detailed dimensions of the riser and downcomer are illustrated in Figure 4.1.

4. Glass tube

Two glass tubes are fixed in the riser and downcomer near to the condenser. The main purpose is for visualization of the flow regimes as well as for monitoring any fluctuation of the flow in the thermosyphon.

5. Measuring equipments

• The Input heat flux is determined by measuring the voltage and the resistance of each heater using a Fluke 45 Dual Multi-meter, and by applying ohms law ($P = V^2/R$), the input heat flux is calculated.

Figure 4.9 shows the potentiometer, solid state relay, and voltmeter which

are used to measure and calibrate the input heat flux to the evaporator channels as well as the two cartridge heaters which normally hidden inside the heaters holes.
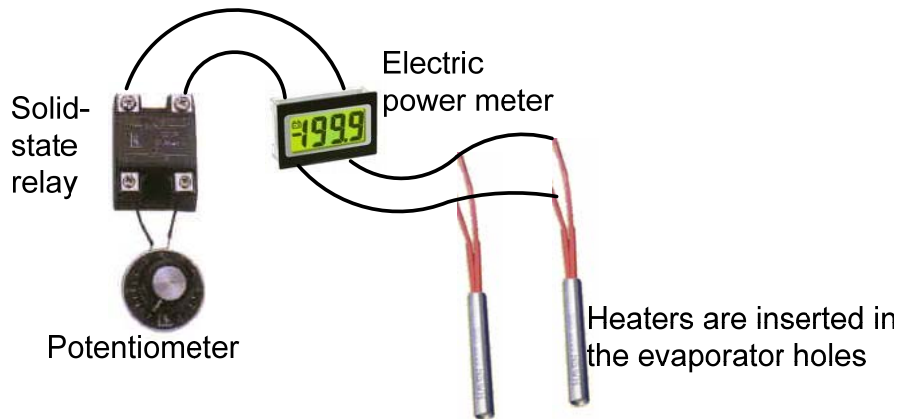
Figure 4.9: Description to input heat flux measurement components with cartridge heaters used in the experiment

In each measurement, the average values are considered in order to eliminate the voltage fluctuations, which is less than 2%.

• Temperature: Seven K-type thermocouple sensors are attached in the thermosyphon system to monitor the temperatures all over the system. The position of each sensor is illustrated in the schematic diagram of the thermosyphon system shown in Figure 4.1.

The temperatures readings are manually registered by multi channels thermometer (Lutron Model: TM-946).

Figure 4.10 illustrate the four channels thermometer (Lutron Model: TM-946) used in the experiment with the K-type thermocouple sensor

Figure 4.10: The four channels thermometer (Lutron Model: TM-946) with K-type thermocouple sensor used in the experiments

- Pressure: Four gauge pressures are used to read the pressures on the inlets and outlets of the evaporator and condenser, Figure 4.1 shows the position of each pressure gauge and Figure 4.11 illustrates the gauge pressure used in the experiment.

Figure 4.11: Gauge pressure used in the experiment

The pressure readings are registered manually, and the corresponding saturation temperature is found manually using saturated liquid vapor tables for each refrigerant.

6. Working fluid

When charging the thermosyphon loop with the working fluid, the non-condensable gases such as air must be removed because it degrades thermosyphon performance.

During charging, the thermosyphon loop is brought to full operation by heating the evaporator chamber. Once the thermosyphon is in full operation, the non-condensable (air) is pushed to the elevated condenser where it is relieved through a valve. This process is repeated until all non-condensable gases are removed from the system. Losses of some of the working fluid occurs during this procedure.

Two types of working fluids are investigated in this study:

- R134a-tetrafluroethane (CF_3CH_2F).

- R22-monochlorodifluoromethane ($CHCLF_2$).

Table 4.1 presents the properties of each fluid.

Table 4.1: Thermodynamic Properties of R134a and R22. Çengel (2003)

	Refrigerant	
	R134a	R22
Boiling temperature (^{o}C)	-26.1 @ 0.1MPa	-40.8 @ 0.1MPa
Critical Temperature (^{o}C)	101.05	96
Critical Pressure (MPa)	4.059	4.936

4.2 Experiment Procedure

The procedure of the experiments are developed to investigate the performance of two-phase thermosyphon system shown in Figure 4.1, which can be used to cool electronic devices that dissipate high heat flux. The heat flux, design of the evaporator, and the type of the refrigerant are the main parameters that believed to affect the performance of such system. These parameters are investigated in details in this experimental works. Moreover, the effect of cooling mode in the condenser is also studied by using both natural and forced convection. The forced convection mode is achieved by fixing a fan to the condenser with velocity of 2.57 m/s and mass flow of 0.083 kg/s.

The system is pressurized with air and all fittings and pipes are tested for leakage by soap foam. Special relief and filling valves are mounted on the system for refrigerant charging and degassing. The liquid refrigerant vigorously boiled for 20 minutes before the valve is opened to exile the air from the system. This degassing procedure minimizes the amount of air dissolved in the fluid to ensure a saturated liquid-vapor closed system.

After the system reaches the room temperature, the initial heat input applied to evaporator is set at 3.9W or 8.2W depending on the test conditions. No data are taken until a steady state condition is reached.

The heat input increments to the evaporator is approximately 5W and beyond 10W at some test conditions, same procedure is followed for each heat flux input.

The maximum heat input to the evaporator throughout the experiments is varied from 40W to about 450W and this mainly depends on the critical heat

flux (CHF).

4.3 Recording Data

The input heat flux, the temperature and pressure at different positions in the system is the main data of interest. These data are obtained or calculated as follows:

1. The input heat flux is calculated using the following equation:

$$\mathbf{P_{heat}} = \mathbf{Q_{in}} = \frac{\mathbf{V^2}}{\mathbf{R}} \tag{4.1}$$

The value of the voltage is measured using voltmeter and the value of the heaters resistors are known from the manufacturer. The value of the resistor is insensitive over a considerable range of temperature (100˚C) since the temperature coefficient of resistance is very low.

The initial heat input is set at 3.9W and incremented in steps to reach 450W in some cases.

2. The temperature is measured continuously from different parts of the system using the thermocouples and thermometers.

The temperatures are then recorded at 10 seconds intervals for two to three minutes, the average temperature are then used in the calculation. The ambient temperature is measured separately at different locations near the evaporator and the condenser by two channels thermometer.

3. The pressure is manually measured in the cycle by four pressure gauges distributed in the system as shown in Figure 4.1.

CHAPTER FIVE

EXPERIMENTAL RESULTS

This chapter summarizes the results of the experiments performed on the thermosyphon system.

The tests are carried out at different conditions:

• Two evaporators are investigated and each evaporator's characteristics are illustrated in chapter 4.

• Two types of refrigerants and different doses are tested.

• Two modes of condensation are tested, natural and forced convection.

The heat flux, amount of refrigerant and reduced pressure are the manipulated parameters in the system.

Each experiment results with its test conditions are shown below.

5.1 Experiment no. 1

This experiment is performed in order to study the thermal performance of thermosyphon system upon the test conditions given in Table 5.1. The input heat flux is varied from 3.9W to 40.2W.

Table 5.1: Experiment no. 1 testing condition

Evaporator design	Evaporator-1
Refrigerant	134a
Refrigerant weight	94g
Reduced Pressure	0.117
Condenser cooling	NC

Table 5.2 illustrates the results obtained taking into account that each reading is averaged from at least four measurements.

Table 5.2: Experiment no. 1 results

Power Q(W)	Pressure (kPa)	Temperature (ºC)						
		Te	Te-in	Te-out	Tc-in	Tc-out	Tamb	Te - Tamb
3.9	560	28.0	23.3	23.5	22.2	22.1	20.0	8.0
8.2	600	35.0	28.8	28.9	26.8	26.0	20.0	15.0
13.8	800	44.3	37.0	37.6	34.3	33.0	20.0	24.3
17.3	860	49.4	41.1	40.9	38.4	36.5	20.0	29.4
21.2	960	54.0	44.7	44.2	41.8	40.0	20.0	34.0
25.4	1050	57.4	46.8	46.0	44.8	42.8	20.0	37.4
29.9	1150	59.7	48.3	48.1	46.1	44.3	20.0	39.7
34.9	1200	65.2	50.1	51.2	48.3	48.0	20.0	45.2
40.2	1250	67.2	52.1	52.3	48.8	48.2	20.0	47.2

Te : evaporator temperature.

Te-in: evaporator's fluid inlet temperature.

Te-out: evaporator's fluid outlet temperature.

Tc-in: condenser's fluid inlet temperature.

Tc-out: condenser's fluid outlet temperature.

Tamb: ambient temperature.

5.2 Experiment no. 2

This experiment is performed in order to study the thermal performance of thermosyphon system upon the test conditions given in Table 5.3. The input heat flux is varied from 3.9W to 46W.

Table 5.3: Experiment no.2 testing condition

Evaporator design	Evaporator-1
Refrigerant	134a
Refrigerant weight	296g
Reduced Pressure	0.135
Condenser cooling	NC

Table 5.4 illustrates the results of experiment no.2.

Table 5.4: Experiment no.2 results

Power Q(W)	Pressure (kPa)	Temperature (°C)						
		Te	Te-in	Te-out	Tc-in	Tc-out	Tamb	Te - Tamb
3.9	650	26.1	19.8	22.0	21.7	20.4	20.0	6.1
8.2	750	30.9	22.4	26.3	26.0	24.0	20.0	10.9
13.8	850	35.0	26.7	32.3	31.5	29.0	20.0	15.0
17.3	920	38.5	28.7	34.6	34.4	31.6	20.0	18.5
21.2	1000	41.8	31.4	37.8	37.6	34.4	20.0	21.8
25.4	1050	44.6	34.4	40.2	40.0	36.6	20.0	24.6
29.9	1100	46.3	35.3	39.2	38.8	35.4	20.0	26.3
34.9	1150	49.2	39.0	43.5	43.1	39.1	20.0	29.2
40.2	1190	49.4	40.5	43.8	44.0	40.0	20.0	29.4
46.0	1200	51.8	42.0	45.0	44.5	40.0	20.0	31.8

5.3 Experiment no. 3

This experiment is performed in order to study the thermal performance of thermosyphon system upon the test conditions given in Table 5.5. The input heat flux is varied from 3.9W to 52.1W.

Table 5.5: Experiment no.3 testing condition

Evaporator design	Evaporator-1
Refrigerant	134a
Refrigerant weight	300g
Reduced Pressure	0.157
Condenser cooling	NC

Table 5.6 illustrates the results of experiment no.3.

Table 5.6: Experiment no.3 results

Power Q(W)	Pressure (kPa)	Temperature (°C)						
		Te	Te-in	Te-out	Tc-in	Tc-out	Tamb	Te - Tamb
3.9	670	25.3	20.2	21.4	20.3	19.4	20.0	5.3
8.2	720	31.0	22.4	24.2	22.5	20.0	20.0	11.0
13.8	810	33.4	26.2	28.4	26.7	23.2	20.0	13.4
17.3	920	37.2	29.2	31.8	29.7	24.4	20.0	17.2
21.2	1000	40.8	32.2	35.0	32.1	28.3	20.0	20.8
25.4	1100	45.0	35.5	39.2	35.0	30.1	20.0	25.0
29.9	1200	48.0	37.9	41.5	37.8	31.2	20.0	28.0
34.9	1250	50.8	39.8	44.4	40.0	33.0	20.0	30.8
40.2	1400	54.1	42.8	47.8	42.8	34.8	20.0	34.1
52.1	1500	57.9	45.7	51.0	43.3	35.0	20.0	37.9

5.4 Experiment no. 4

This experiment is performed in order to study the thermal performance of thermosyphon system upon the test conditions given in Table 5.7. The input heat flux is varied from 3.9W to 155.6W.

Table 5.7: Experiment no.4 testing condition

Evaporator design	Evaporator-1
Refrigerant	134a
Refrigerant weight	400g
Reduced Pressure	0.172
Condenser cooling	NC

Table 5.8 illustrates the results of experiment no.4.

Table 5.8: Experiment no.4 results

Power Q(W)	Pressure (kPa)	Temperature (ºC)						
		Te	Te-in	Te-out	Tc-in	Tc-out	Tamb	Te - Tamb
3.9	750	29.7	24.8	24.5	22.9	22.1	20.1	9.6
8.2	800	32.0	25.5	26.9	23.6	22.1	20.1	11.9
13.5	900	36.5	29.4	31.0	26.8	23.8	20.3	16.2
21.3	1080	43.0	35.4	37.3	31.6	28.1	20.3	22.7
29.9	1280	49.3	40.9	43.0	35.6	31.6	20.4	28.9
40.3	1420	53.7	44.8	47.0	38.4	33.0	20.4	33.3
52.2	1520	56.5	48.1	50.4	40.7	34.7	20.4	36.1
65.6	1770	63.0	53.4	56.5	43.9	35.9	20.4	42.6
80.5	2080	70.0	60.9	64.2	48.8	39.5	20.4	49.6
97.0	2320	74.8	65.2	68.8	52.4	42.4	20.4	54.4
115.0	2600	80.5	69.8	74.0	55.2	43.2	20.6	59.9

Power Q(W)	Pressure (kPa)	Temperature (ºC)						
		Te	Te-in	Te-out	Tc-in	Tc-out	Tamb	Te - Tamb
134.5	2980	87.5	75.9	80.5	59.4	44.0	20.6	66.9
155.6	3280	94.1	80.5	85.8	62.9	45.2	20.6	73.5

5.5 Experiment no. 5

This experiment is performed in order to study the thermal performance of thermosyphon system upon the test conditions given in Table 5.9. The input heat flux is varied from 52.2W to 414.0W.

Table 5.9: Experiment no.5 testing condition

Evaporator design	Evaporator-1
Refrigerant	134a
Refrigerant weight	400g
Reduced Pressure	0.172
Condenser cooling	FC
	$v = 2.57$m/s, $\dot{m} = 0.083$ kg/s

v: forced air velocity (m/s)

$\dot{m}$: Air mass flow (kg/s)

Table 5.10 illustrates the results of experiment no.5.

Table 5.10: Experiment no.5 results

Power Q(W)	Pressure (kPa)	Temperature (ºC)						
		Te	Te-in	Te-out	Tc-in	Tc-out	Tamb	Te - Tamb
52.2	760	30.9	22.9	24.7	21.9	20.5	20.8	10.1
65.6	780	31.8	23.1	25.0	22.1	20.6	20.8	11.0
80.5	790	32.8	23.5	25.6	22.3	20.7	20.9	11.9
97.0	800	33.7	23.8	26.1	22.4	20.7	20.9	12.8
115.0	810	34.4	23.9	26.5	22.5	20.8	20.9	13.5
134.5	810	35.2	24.3	27.2	22.6	20.8	20.9	14.1
155.6	840	36.3	24.7	27.7	22.9	21.0	20.9	15.6
178.2	850	36.8	24.9	28.2	23.0	21.1	20.9	15.9
202.3	860	37.6	25.1	28.7	23.1	21.1	20.9	16.7
230.0	860	38.0	25.4	29.3	23.4	21.1	20.9	17.1
255.2	890	39.4	25.7	29.8	23.5	21.1	20.9	18.5
284.0	900	40.2	26.0	30.3	23.6	21.2	20.9	19.3
315.0	930	41.8	26.2	30.7	23.7	21.2	21.0	20.8
346.0	960	43.3	26.9	32.0	24.0	21.2	21.0	22.3
414.0	1000	44.5	27.8	34.0	25.5	21.3	21.1	23.4

5.6 Experiment no. 6

This experiment is performed in order to study the thermal performance of thermosyphon system upon the test conditions given in Table 5.11. The in-put heat flux is varied from 5.8W to 115.0W.

Table 5.11: Experiment no.6 testing condition

Evaporator design	Evaporator-1
Refrigerant	R22
Refrigerant weight	400g
Reduced Pressure	0.182
Condenser cooling	NC

Table 5.12 illustrates the results of experiment no.6.

Table 5.12: Experiment no.6 results

Power Q(W)	Pressure (kpa)	Temperature (ºC)						
		Te	Te-in	Te-out	Tc-in	Tc-out	Tamb	Te - Tamb
5.8	950	24.3	20.3	21.5	20.6	19.9	20.0	4.3
8.12	1080	30.4	26.2	27.1	26.4	25.5	20.0	10.4
13.8	1220	35.4	30.5	31.7	31.1	29.3	20.0	15.4
21.1	1350	39.8	34.8	35.7	35.2	32.7	20.0	19.8
29.9	1550	45.0	39.9	41.0	39.6	36.3	20.0	25.0
40.2	1820	52.2	46.9	48.1	46.1	41.6	20.0	32.2
52.1	2100	58.7	53.1	54.2	51.4	46.0	20.0	38.7
65.5	2350	63.6	57.2	58.6	55.5	49.6	20.0	43.6
80.5	2700	71.5	63.4	65.4	59.4	46.9	20.0	51.5
96.9	2950	74.8	66.0	68.3	61.4	52.0	20.0	54.8
115.0	3250	80.5	70.4	73.5	65.4	54.4	20.0	60.5

5.7 Experiment no. 7

This experiment is performed in order to study the thermal performance of thermosyphon system upon the test conditions given in Table 5.13. The input heat flux is varied from 52.2W to 417.0W.

Table 5.13: Experiment no.7 testing condition

Evaporator design	Evaporator-1
Refrigerant	R22
Refrigerant weight	400g
Reduced Pressure	0.182
Condenser cooling	FC
	v =2.57m/s, ṁ = 0.083 kg/s

Table 5.14 illustrates the results of experiment no.7.

Table 5.14: Experiment results no. 7

Power Q(W)	Pressure (kPa)	Temperature (°C)						
		Te	Te-in	Te-out	Tc-in	Tc-out	Tamb	Te - Tamb
52.2	1010	28.3	23.1	23.3	22.7	22.5	20.0	8.3
65.6	1040	29.2	23.4	23.8	23.1	23.8	20.0	9.2
80.5	1050	30.1	23.7	24.4	23.5	23.3	20.0	10.1
97.0	1050	31.0	23.8	24.6	23.3	23.0	20.0	11.0
115.0	1060	31.8	24.1	25.1	23.4	22.3	20.0	11.8
134.5	1090	33.2	24.7	25.4	23.7	22.5	20.0	13.2
155.6	1100	33.3	24.6	26.0	23.8	22.5	20.0	13.3
178.2	1110	34.3	24.9	26.5	24.0	22.3	20.0	14.3
202.3	1150	35.3	25.1	27.1	24.2	22.3	20.0	15.3
230.0	1160	36.3	25.4	27.6	24.3	22.0	20.0	16.3
255.2	1190	37.5	25.8	28.3	24.5	21.9	20.0	17.5
284.0	1200	38.3	25.7	28.8	24.8	22.0	20.0	18.3
314.0	1220	39.1	26.4	29.1	24.9	21.8	20.0	19.1
417.0	1250	40.3	27.0	30.3	25.3	21.7	20.0	20.3

5.8 Experiment no. 8

This experiment is performed in order to study the thermal performance of thermosyphon system upon the test conditions given in Table 5.15. The input heat flux is varied from 8.2W to 346.0W.

Table 5.15: Experiment no.8 testing condition

Evaporator design	Evaporator-2
Refrigerant	R134a
Refrigerant weight	400g
Reduced Pressure	0.182
Condenser cooling	NC

Table 5.16 illustrates the results of experiment no.8.

Table 5.16: Experiment results no. 8

Power Q(W)	Pressure (kpa)	Temperature (°C)						
		Te	Te-in	Te-out	Tc-in	Tc-out	Tamb	Te - Tamb
8.2	750	31.0	24.4	20.8	22.5	21.8	25.0	6.0
13.5	800	34.6	27.8	27.4	24.7	22.2	25.0	9.6
21.3	950	37.4	31.0	31.0	29.0	27.3	25.0	12.4
29.9	1200	48.4	41.6	41.6	40.6	38.8	25.0	23.4
52.2	1300	52.6	43.3	44.1	42.8	41.9	25.0	27.6
80.5	1700	63.8	50.9	53.4	52.0	48.9	25.0	38.8
97.0	1800	66.8	49.9	55.0	52.9	52.0	25.0	41.8
115.0	2000	74.0	52.5	59.9	57.7	52.9	25.0	49.0
134.5	2500	82.2	64.3	70.0	67.9	64.4	25.0	57.2
155.6	2600	85.9	69.1	72.9	70.5	67.5	25.0	60.9

Power Q(W)	Pressure (kpa)	Temperature (°C)						
		Te	Te-in	Te-out	Tc-in	Tc-out	Tamb	Te - Tamb
178.2	2700	79.5	72.8	75.6	72.9	70.4	25.0	54.5
202.3	2950	96.0	79.0	81.0	78.0	76.0	25.0	71.0
230.0	3150	98.9	80.4	82.0	79.0	76.8	25.0	73.9
255.2	3200	101.0	82.0	84.0	81.7	80.3	25.0	76.0
284.0	3400	103.6	84.4	86.4	83.6	81.3	25.0	78.6
346.0	3500	106.0	86.9	84.1	85.8	83.9	25.0	81.0

5.9 Experiment no. 9

This experiment is performed in order to study the thermal performance of thermosyphon system upon the test conditions given in Table 5.15. The input heat flux is varied from 8.2W to 178.2W.

Table 5.17: Experiment no.9 testing condition

Evaporator design	Evaporator-2
Refrigerant	R22
Refrigerant weight	400g
Reduced Pressure	0.182
Condenser cooling	NC

Table 5.18 illustrates the results of experiment no.9.

Table 5.18: Experiment results no. 9

Power Q(W)	Pressure (kpa)	Temperature (°C)						
		Te	Te-in	Te-out	Tc-in	Tc-out	Tamb	Te - Tamb
8.2	1050	28.0	24.4	23.7	24.2	24.2	24.8	3.2
13.5	1180	31.5	26.8	27.8	27.8	27.8	24.8	6.7
21.3	1250	34.4	30.0	30.6	30.0	29.8	24.8	9.6
29.9	1300	37.2	31.7	31.1	31.2	30.8	24.8	12.4
65.6	1600	47.2	38.6	40.4	39.1	38.7	24.8	22.4
80.5	1700	51.4	40.7	45.2	43.4	42.8	24.8	26.6
97.0	2100	59.0	50.6	52.5	50.7	49.3	24.8	34.2
115.0	2400	69.2	51.9	56.0	53.4	52.4	24.8	44.4
134.5	2500	73.6	55.8	60.0	57.2	56.2	24.8	48.8
155.6	2600	76.0	57.4	60.8	58.0	56.8	24.8	51.2
178.2	3000	90.7	67.5	70.2	67.1	65.0	24.8	65.9

CHAPTER SIX

RESULTS ANALYSIS & DISCUSSION

The performance of the designed two-phase thermosyphon system is studied and analyzed based on the following factors:

6.1 Experimental Heat Transfer Coefficient

The experimental heat transfer coefficient is defined by the ratio of the heat flux and the temperature difference between the evaporator wall and the saturation temperature of the refrigerant as in Equation (6.1). Since it is difficult to measure the surface temperature of the channels, it is assumed that the temperature of the inner channel surface is the same as the temperature measured inside the wall nearby the channel.

$$\mathbf{h}_{exp} = \frac{\mathbf{Q/A}}{\mathbf{T}_e - \mathbf{T}_{sat}} \approx \frac{\mathbf{Q/A}}{\mathbf{T}_s - \mathbf{T}_{sat}} \qquad (6.1)$$

The heat transfer coefficient is affected by errors in the temperature difference between the wall and the fluid and in the heat flux measurement. This temperature difference is compensated in the above equation by subtracting it from temperature difference between the evaporator wall and the saturation temperature of the refrigerant; it is measured and was found to be neglected from the estimation. (R. Khodabandeh and B. Palm, 2002)

High heat transfer coefficient is greatly depending on the temperature difference between the evaporator wall and the temperature of the refrigerant in the inside channels.

The overall heat transfer coefficient is calculated as shown in Equation (6.2).

$$\mathbf{U} = \frac{\mathbf{Q/A}_h}{\mathbf{T}_e - \mathbf{T}_{amb}} \qquad (6.2)$$

The surface area of the heaters attached to the evaporator has a great effect on calculating this coefficient (U) while the surface of the evaporator channels has this effect in calculating the evaporator heat transfer coefficient (h_{exp}) as shown in Equation (6.1).

The heat flux exposed to the evaporator is calculated using Equation (6.3).

$$\textbf{Heat Flux} = \frac{\textbf{Q}}{\textbf{A}} \tag{6.3}$$

The Experimental Heat Transfer coefficient is studied in accordance with the effect of the following factors:

1. The effect of the working fluid.

2. The effect of different evaporator's designs.

3. The effect of different reduced pressures.

6.1.1 Experimental Heat Transfer Coefficients for R134a and R22 at Different Heat Loads Using NC

Figure 6.1 shows the heat transfer coefficient versus the heat load dissipated into the evaporator channels. The experimental data are shown in Tables 5.8 and 5.12. Equation (6.1) is used for calculating experimental heat transfer coefficient. It is clear that the heat transfer coefficient increases with increasing heat load.
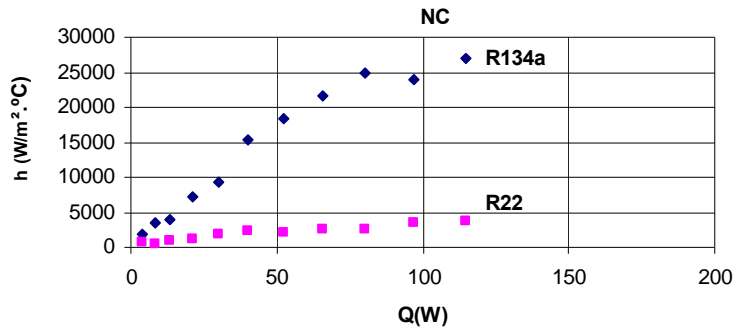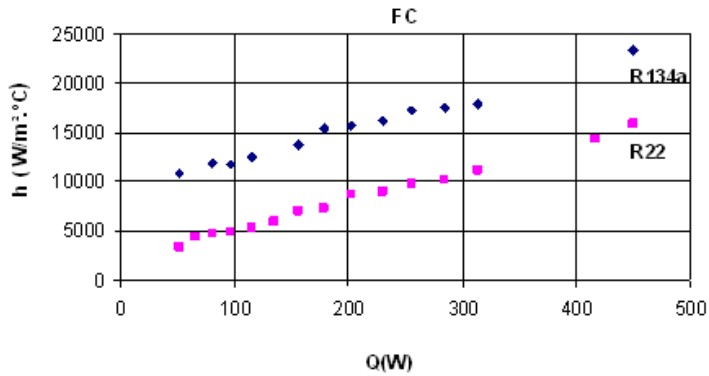
Figure 6.1: Comparison between the heat transfer coefficients for R134a and R22 at different heat loads using evaporator-1 and NC.

The direct proportional relation between the heat transfer coefficient and the heat load indicates nucleate heat transfer boiling in the thermosyphon system.

6.1.2 Experimental Heat Transfer Coefficients for 134a and R22 at Different Heat Loads Using FC

Figure 6.2 illustrates the relation between the heat transfer coefficient and the heat load with forced convection, which proves once again that the heat transfer coefficient increases with heat load. The experimental data are shown in Tables 5.10 and 5.14. Equation (6.1) is used in calculating experimental heat transfer coefficient. The precedence of R134a over R22 is still existed.
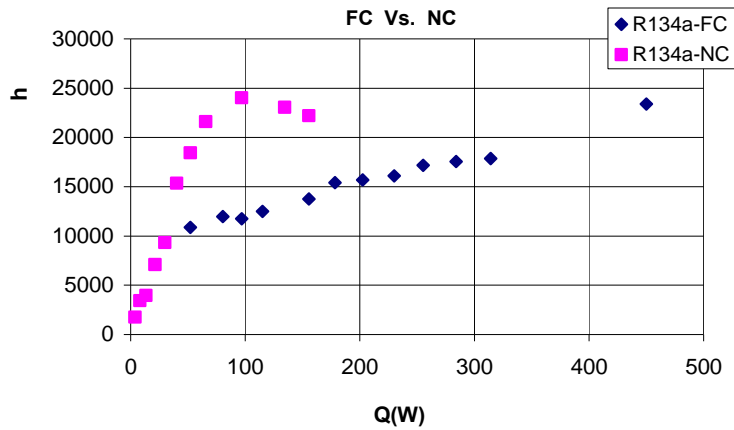
Figure 6.2: Comparison between heat transfer coefficients for R134a and R22 at different heat loads using evaporator-1 and FC.

It is worth noting that the heat load exposed to the evaporator at forced convection is the maximum capacity of the heaters used in the experiment not the maximum capacity of the system.

The heat transfer coefficient with free convection is higher than heat transfer coefficient with forced convection at the same heat load at low heat loads. This is due to higher saturation pressure in the thermosyphon system at natural convection. This fact appears clearly in Figure 6.3, which compares between the forced and natural convection heat transfer coefficients.

The experimental data is shown in Tables 5.8 and 5.10. Equation 6.1 is used in calculating experimental heat transfer coefficient.

Figure 6.3: Comparison between heat transfer coefficients using FC and NC for R134a at different heat loads, and evaporator-1.

R. Khodabandeh, (2004) studied the influence of forced and natural convection cooling of condenser on the heat transfer coefficient between the evaporator wall and refrigerant versus heat flux corresponding to the surface area of the inner tube channels with refrigerant Isobutane (R600a) . He showed that the heat transfer coefficients increase with heat flux; indicate nucleate boiling heat transfer dominance in the system. He showed also the natural convection cooled condenser gives a higher heat transfer coefficient in the evaporator than forced convection cooled condenser.

6.1.3 Experimental Heat Flux Versus Temperature Difference for 134a and R22, Using NC

Figure 6.4 shows the relation between heat flux and the temperature difference between the evaporator wall and the saturation temperature of the refrigerant inside the channels. The experimental data are shown in Tables 5.8 and 5.12. Equation 6.3 is used in calculating heat flux dissipated in the evaporator.
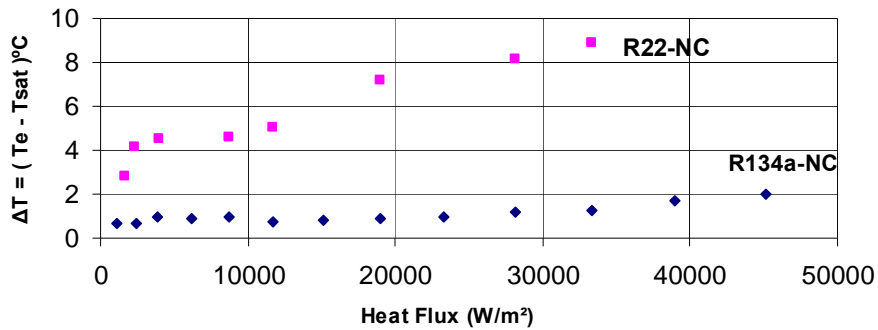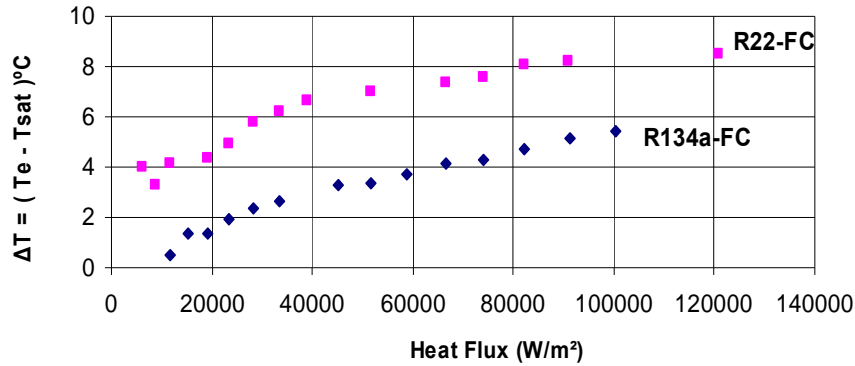
Figure 6.4: Comparison between heat flux for R134a and R22 versus the resulted temperature difference, using evaporator-1 and NC.

At low temperature difference, the maximum heat flux that could be absorbed in the evaporator channels using R134a is higher than that of R22, which affirm the preference of R134a under this test conditions.

6.1.4 Experimental Heat Flux versus Temperature Difference for R134a and R22, Using FC

Figure 6.5 illustrates the relation between heat flux and heat load at forced convection, the experimental data are shown in Tables 5.10 and 5.14. Equation 6.3 is used in calculating heat flux dissipated in the evaporator.

Figure 6.5 indicates that at forced convection the maximum heat flux that could be absorbed by the evaporator is nearly twice; the Figure also shows that both refrigerants establish similar heat flux absorption, but R134a keeps its preference by lower temperature difference.

Figure 6.5: Comparison between heat flux for R134a and R22 versus the resulted temperature difference, using evaporator-1 and FC

The heat flux with free convection is higher than heat flux with forced convection at the same heat load and this due to higher saturation pressure in the thermosyphon system at natural convection.

This fact clearly appears in Figure 6.6, which compares between the forced and natural convection heat flux, the experimental data are shown in Tables 5.8 and 5.10. Equation 6.3 is used in calculating heat flux dissipated in the evaporator.

At forced convection, the capacity of the system increased to higher levels.
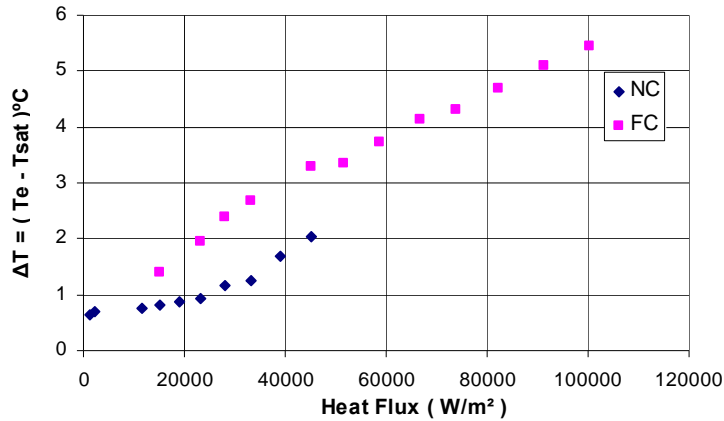
Figure 6.6: Comparison between FC and NC heat flux versus heat load R134a, evaporator-1.

6.1.5 Overall Heat Transfer Coefficient for R134a at Different Heat Loads, Using NC and FC

The overall heat transfer coefficient is calculated by using equation 6.2 and with heaters surface area (A_h = 19.48 cm²).
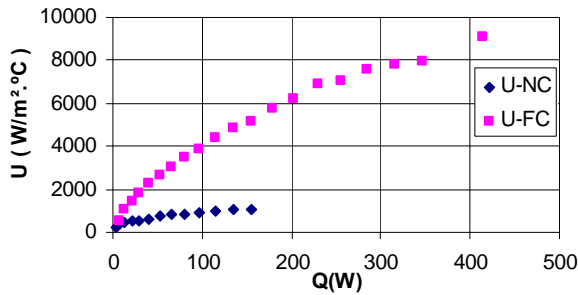
Figure 6.7: Comparison between the overall heat transfer coefficients for R134a at different heat loads using NC and FC.

As seen in Figure 6.7 the overall heat transfer coefficient for forced convection is 9.4 kW/m².˚C at 415W while it is 1.08 kW/m².˚C at 155W.

This is due to efficient condensation at forced convection, which consequently contributes to low thermal resistance between the condenser and

the surrounding. This thermal resistance is greatly depending on the type of convection and the surface area of the condenser.

R. Khodabandeh, (2004) studied the influence of forced and natural convection cooling of condenser on the overall heat transfer coefficient at different heat loads using refrigerant Isobutane (R600a) and at heater surface area (9.53×9.53 mm), he found that the overall heat transfer coefficient for forced convection is 12000 W/m².K at 90W while it was 9500 W/m².K at 70W.

6.1.6 Experimental Heat Transfer Coefficient Using Different Evaporator Design

The heat transfer coefficient is greatly depending on the design of the evaporator channels. In this experiment, both types of evaporators are investigated. The detail design of each evaporator is presented in chapter 4.

The surface area of the channels in the evaporator-2 is 1.45 times larger than the surface area of the channels in evaporator-1.

A comparison between the heat transfer coefficients and heat flux of the thermosyphon system using evaporator-1 and evaporator-2 are given in Figures 6.8 and 6.9, respectively. The experimental data is presented in Tables 5.4 and 5.8.
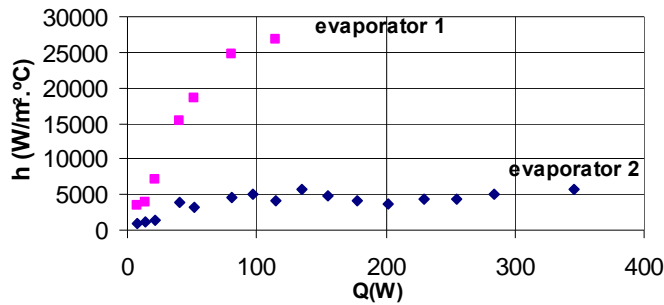
Figure 6.8: Comparison between heat transfer coefficients of evaporator-1 and evaporator-2 for R134a at different heat loads, using NC.

As previously stated, the heat transfer depends on the surface area, the heat transfer coefficient, and the temperature difference. Usually increasing the heat transfer area results higher heat transfer. However, one should not forget that the channels diameters affect the heat transfer coefficient, so in order to determine the effect of the area, the two evaporators should have be manufactured with different surface areas but with same channels diameter, i.e. by adding new channels, which is not the case of this study.

Figure 6.9 compares between the absorbed heat flux of the evaporator-1 and evaporator-2. At high temperature difference the performance of evaporator-2 is better than evaporator-1 but at higher temperature difference.
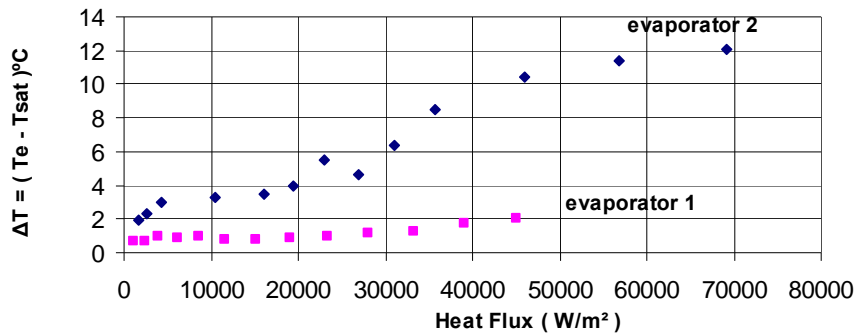
Figure 6.9: Comparison between heat transfer coefficients of evaporator-1 and evaporator-2 for R134a at different heat loads.

6.1.7 Experimental Heat Transfer Coefficient at Different Heat Loads and   Reduced Pressures

Figure 6.10 illustrates the relationship between the heat transfer coefficient and the heat load at different reduced pressures; the experimental data are shown in Tables 5.2, 5.4, and 5.6.

Figure 6.10 shows that, the heat transfer coefficient increases as the reduced pressure increases at different heat loads. This result has been approved by many researchers who studied the effect of pressure on the boiling heat transfer coefficient. (Cooper, M. G., 1984), (Gorenflo, D., 1993), and (R. Khodabandeh, B. Palm, 2002)

This result is not restricted for R134a, but it is applicable to different fluids because the law of corresponding states that variation of thermodynamic and transport properties with reduced pressure is similar for different fluids. (Khodabandeh and Palm 2002)
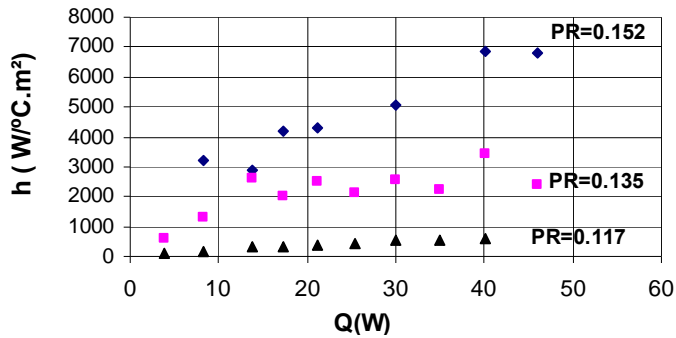
Figure 6.10: Comparison between heat transfer coefficients for different reduced pressures at different heat loads, using evaporator-1 and R134a.

Figure 6.11 illustrates more clearly the relation between the heat transfer coefficient and the reduced pressure at specific heat load range.
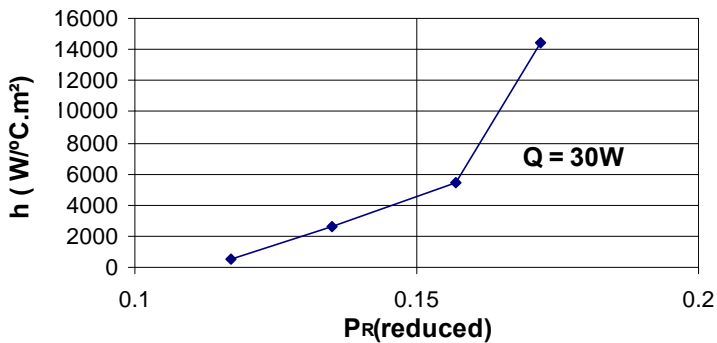
Figure 6.11: Comparison between heat transfer coefficients at different reduced pressure for R134a, using evaporator-1.

From Figures 6.10 and 6.11 the heat transfer coefficient is promoted by increasing reduced pressure. Several investigators have studied the effect of the pressure level on the heat transfer coefficient and proved the similar phenomenon with different refrigerants. (Bao, Z. Y et al, 2000), (Steiner, D. and J. Taborek, 1992), and (Klimenko, V.V 1990).

The relationship between the heat flux and temperature difference at dif-

ferent reduced pressures is presented in Figure 6.12.
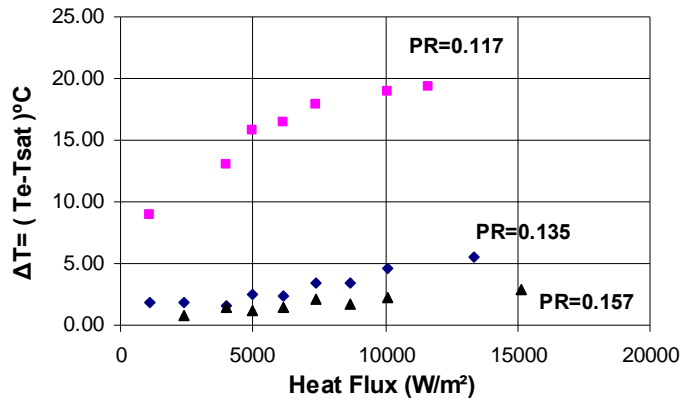
Figure 6.12: Relationship between the heat flux and temperature difference at reduced pressures using evaporator-1 and R134a.

It is clear that as the heat flux increases the temperature difference increases but with different slopes depending on the saturation pressure in the thermosyphon system, so the heat transfer coefficient increases with increasing saturation pressure, see Figure 6.11.

At reduced pressures 0.157 and 0.135, the maximum temperature difference obtained is 2.9°C at 15.2 kW/m² and is 5.51°C at 13.4 kW/m², respectively.

R. Khodabandeh, B. Palm (2002) studied the effect of reduced pressure on the temperature difference at different heat flux, using refrigerant Isobutane (R600a). They found that the temperature difference decreases as the reduced pressure increases, while the temperature difference increases as the heat flux increases. The maximum obtained temperature difference was 7.5°C at 300 kW/m² and was 22°C at 275 kW/m² with reduced pressure 0.3 and 0.02, respectively.

6.2 Temperature Difference

The temperature difference between the evaporator wall and the refrigerant is a factor of a great importance in determining the performance of the system, since the evaporator section is ordinary exposed to high heat flux compared to other parts of the system.

The main goals of most researchers who studied in the thermosyphon cooling systems is to achieve low temperature difference and consequently high heat transfer coefficient.

The effect of the following factors on the temperature difference is investigated in this work and the results are discussed in following section:

6.2.1 The Effect of Refrigerant Type on the Temperature Difference at Different Heating Loads, Using NC.

Figure 6.13 presents the relationship between the heat load and the measured temperature difference between the surface of the evaporator and the operating liquid. The experiment is conducted using refrigerants R134a and R22 at natural convection. The experimental data are shown in Tables 5.8 and 5.12.
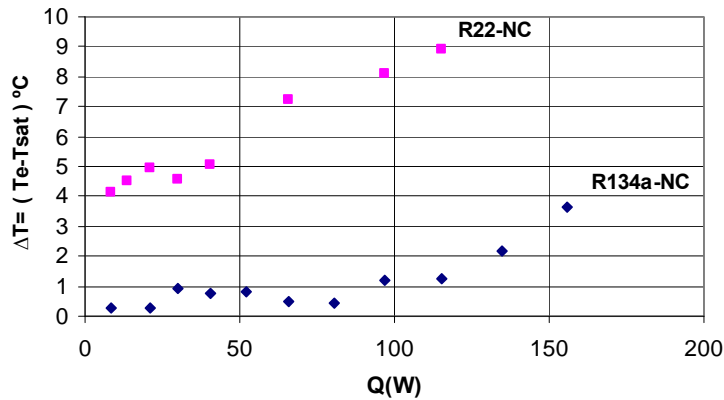
Figure 6.13: Temperature difference vs. heat loads using evaporator-1 and NC.

It is clear from the figure that the temperature difference did not exceed 1⁰C for heating load of 100W for R134a. The temperature difference increases rapidly with heat load and exceeded 8⁰C for the same heating load of R22. So far, the temperature difference is found to be highly dependant on the refrigerant type, the heat load, and the reduced pressure. The effect of refrigerant type and the reduced pressure is pronounced more than the heat load as can be seen from Figure 6.13 and 6.12.

6.2.2 The Effect of Refrigerant Type on the Temperature Difference at Different Heating Loads, Using FC.

Figure 6.13 shows relation of the temperature difference for the refrigerants R134a and R22 versus heat load with forced convection condensation. The experimental data are shown on Tables 5.10 and 5.14.
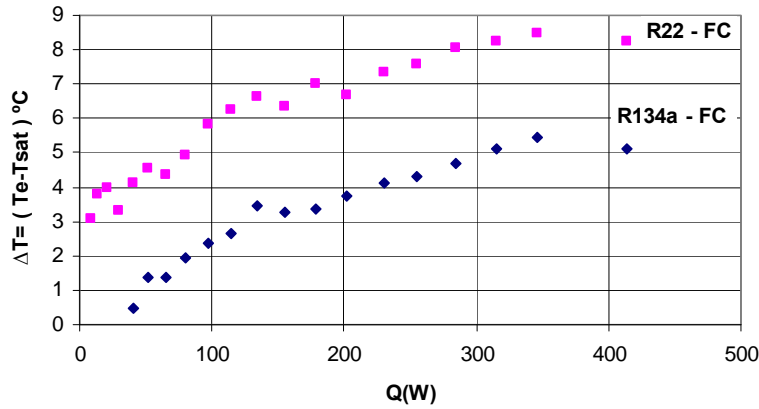
Figure 6.14: Temperature difference vs. heat loads using evaporator-1 and FC.

It is worthy to note the temperature difference of natural convection is slightly lower than that of forced convection as shown in Figure 6.15. The experimental data are shown on Tables 5.8 and 5.10.
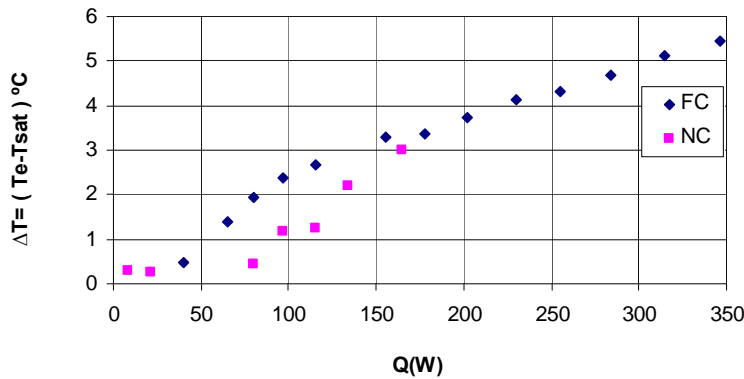
Figure 6.15: Comparison between temperature difference for NC and FC at different heat loads using R134a and evaporator-1.

Using natural convection condensation is better than using forced convection condensation at low heat loads because of the low temperature difference involved at natural convection, so increasing the surface area of the condenser, if possible, could be preferable than using forced convection.

However, at high heating loads forced convection should be presented.

6.2.3 Temperature difference as a function of reduced pressure at different ranges of heat load

Figure 6.16 illustrates the relation of temperature difference versus reduced pressure at different heat load. The experimental data are shown in Tables 5.2, 5.4 and 5.6.

Figure 6.16 shows two things, a steady increase in the temperature difference with increasing heat input and shows a decrease in the temperature difference as the reduced pressure increases. The Figure also shows that as the reduced pressure increases the temperature differences at different heat loads become relatively smaller than that at lower reduced pressure.
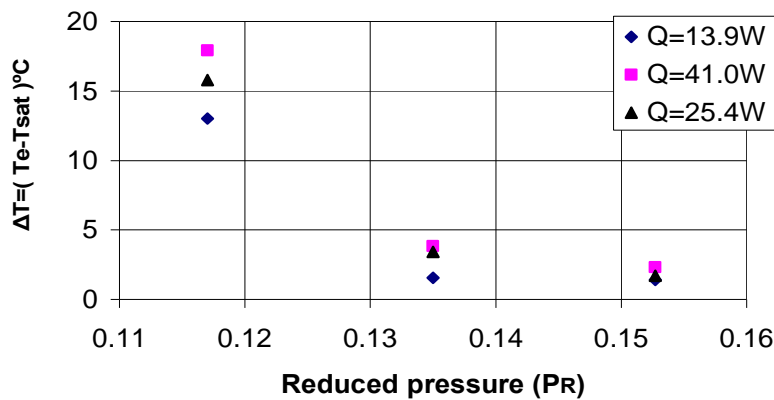
Figure 6.16: Temperature difference vs. reduced pressure for evaporator-1, and R134a.

R. Khodabandeh, B. Palm (2002) studied the effect of pressure on the temperature difference for different heat loads, using refrigerant Isobutane (R600a). They showed clearly that the temperature difference increases as the reduced pressure decreases and showed that a steady increase in the

temperature difference with increasing heat input.

6.3 Thermal Resistance and Temperature Distribution in the Thermosyphon System

The lower thermal resistance in the system is a factor of interest in evaluating the performance of thermosyphon system. The high amounts of dissolved gases in the system probably contribute to high thermal resistance. The dissolved gases reduce the heat transfer coefficient, which consequently lead to a decrease in critical heat flux.

The overall thermal resistance of the thermosyphon system is defined as

$$\frac{1}{U.A_h} = \frac{T_e - T_{amb}}{Q} \tag{6.4}$$

There are different types of thermal resistances in the thermosyphon system, which has great effect on the performance of the system. Of these resistances one can highlight some of them as the following: (R. Khodabandeh, 2004)

- The thermal resistance between the cylindrical heaters which represent the heat source and the temperature inside the channels of the evaporator, this resistance should be small as much as possible for a good design.

For this purpose, in this study cylindrical holes with diameters and height equal to that of the heaters are drilled vertically in the evaporator and parallel to the cooling channels. The heaters are tightly embedded in the evaporator walls. In order to eliminate the possible contact resistance, a high thermal conductivity special epoxy is placed between the heaters and the evaporator walls.

- The thermal resistance between the saturated refrigerant in the condenser and the outer condenser surface is the sum of condensing thermal resistance inside the condenser and conduction thermal resistance from the inside to the outside of the condenser wall.

- The thermal resistance between the outer condenser surface and the ambient air. This thermal resistance is highly dependent on the type of cooling of the condenser; natural or forced convection.

- The thermal resistance between the thermocouple in the evaporator from the inside vertical channels and the liquid bulk temperature consists of the heat conduction resistance and the boiling resistance in the evaporator channels. This resistance is the most important resistance in the design for the performance of an advanced thermosyphon loop. This resistance can be large or small depending on the design and choice of working fluid. The evaporator resistance increases when a part of the evaporator channel area is not in direct contact.

- The last resistance is caused by the pressure difference, which exists between the evaporator and the condenser. This resistance will increase by any conditions in two phase flow that increase the flow pressure drop such as higher vapor quality and smaller diameter tubing.
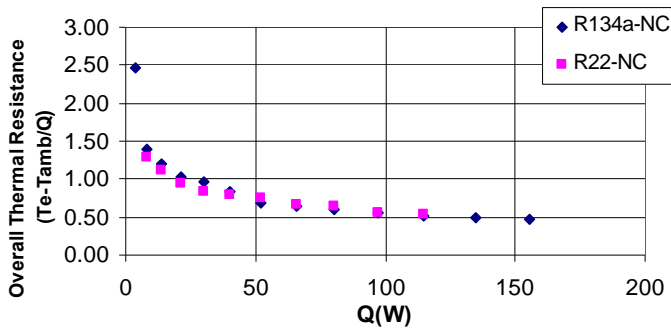
The overall thermal resistance which is equal to the sum of the above thermal resistances will be investigated.

The following discussion and analysis illustrates the effects of using forced and natural convection condensation in the condenser, different heat loads and different refrigerants on the thermal resistance and the temperature dis-

tribution in the thermosyphon system.

6.3.1 Overall Thermal Resistance at Different Heat Loads for R134a and R22 Using NC

Figure 6.17 below illustrates the effect of different heat loads on the thermal resistance using R134a and R22 at natural convection condensation. The experimental data are shown in Tables 5.8 and 5.12. Equation 6.4 is used in calculating overall thermal resistance in the thermosyphon system.

Figure 6.17: Overall thermal resistance at different heat loads for R134a and R22, using evaporator-1 and NC

The refrigerant has no effect on the overall thermal resistance; i.e. overall thermal resistance is independent on the operating refrigerant.

The overall thermal resistance is exponentially decaying with heat loads

6.3.2 Overall Thermal resistance at Different Heat Loads for R134a and R22 Using FC

Figure 6.18 illustrates the effect of different heat loads on the thermal resistance using R134a and R22 for forced convection condensation. The experimental data are shown in Tables 5.10 and 5.14. Equation 6.4 is used in

calculating overall thermal resistance in the thermosyphon system.

Figure 6.18: Overall thermal resistance at different heat loads for R134a and R22, using evaporator-1 and FC
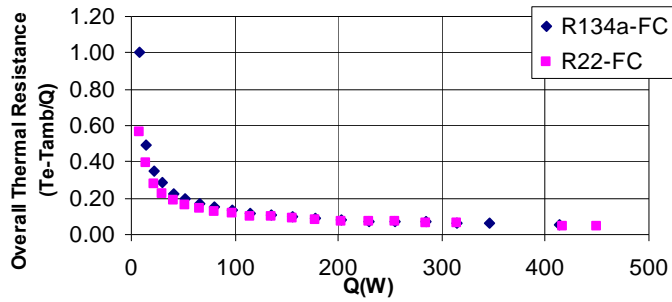
Figure 6.18 shows that for free convection, the overall thermal resistance is independent on the operating refrigerant and it is exponentially decaying with the heat load.

From the previous discussion and analysis of Figures 6.17 and 6.18, it is clear that with forced convection condensation a lower thermal resistance can be achieved in the thermosyphon system than natural convection condensation.

Figure 6.19 summarizes the above discussion and illustrates more clearly the behavior of the overall thermal resistance with respect to the type of condenser cooling of R134a. The overall thermal resistance is a function of type of condenser cooling, since the resistance between the outer condenser surface and the ambient air has great effect on the overall thermal resistance.
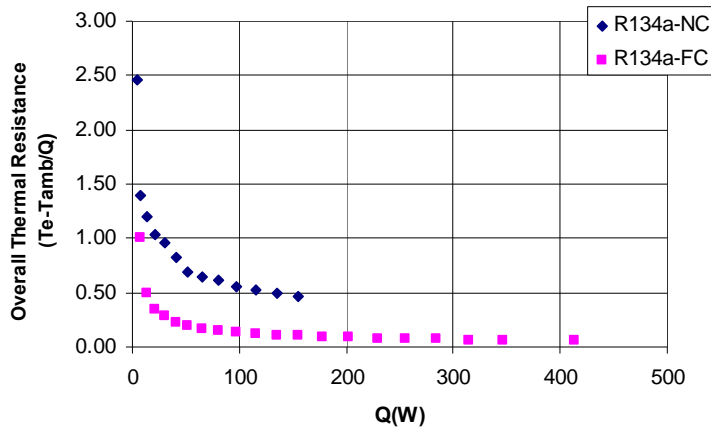
Figure 6.19: Comparison between Overall thermal resistance Using NC and FC at different heat loads for R134a using evaporator-1

R. Khodabandeh, (2004) studied the influence of forced and natural convection cooling of condenser on the overall thermal resistance at different heat loads, using refrigerant Isobutane (R600a) and he found that the overall thermal resistance is decreased with heating load on both natural and forced convection condenser cooling, he also found that at natural convection cooled condenser arrangement a higher overall thermal resistance than that of forced convection. The minimum value of overall thermal resistance was found to be 0.9°C/W at 90W and 1.15°C/W at 70W at forced and natural convection, respectively.

6.3.3 Temperature Distribution in the Thermosyphon System at Different Heat Loads for R134a Using NC Condensation

Figure 6.20 shows the distribution of the temperature at different locations of the thermosyphon system using R134a with natural convection. The experimental data is shown in Table 5.8.
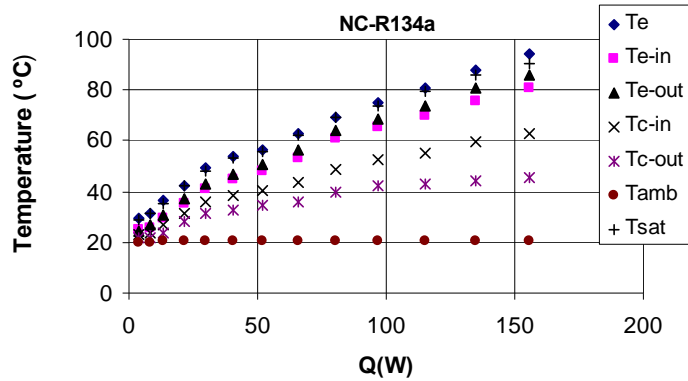
Figure 6.20: Temperature distribution at different heat loads for R134a using evaporator-1 and NC condensation.

6.3.4 Temperature Distribution in the Thermosyphon System at Different Heat Loads for R134a Using FC Condensation

Figure 6.21 shows the distribution of the temperatures at different locations of the thermosyphon system using R134a and forced convection. The experimental data are shown in Tables 5.10.
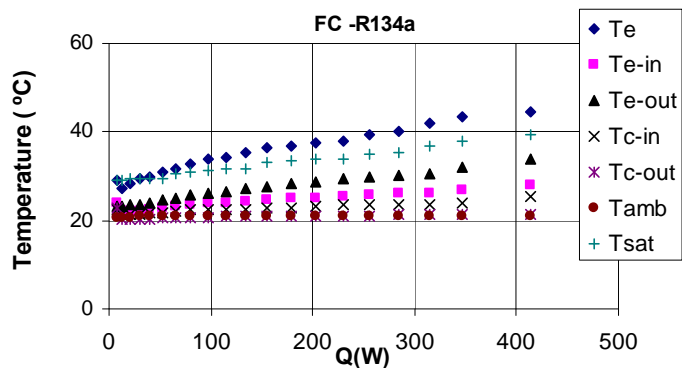
Figure 6.21: Temperatures distribution at different heat loads for R134a using evaporator-1 and FC.

At natural convection (Figure 6.20) at heat load above 150W, the evaporator temperature reaches high temperature value of 94°C while at forced

convection (Figure 6.21) it reaches 42˚C at 420W.

This phenomenon is applied for all temperatures at different locations in the thermosyphon system. This is due to lower and steady saturation temperature (30-40˚C) in the condenser in case of forced convection. While at natural convection, the saturation temperature is increasing rapidly with heating load (21-71˚C).

The effect of the thermal resistances on the behavior of the thermosyphon system is highlighted more clearly in Figures 6.20 and 6.21. For example, Figure 6.20 illustrates the temperature distribution at natural convection condensation shows that the difference between the temperatures of the evaporator input and condenser input is 17°C. This difference is mainly caused by the effect of thermal resistance on the system.

Figure 6.21 shows that the difference between the temperatures of the evaporator input and condenser input becomes lower which is 9°C. this relatively small difference caused from associated low thermal resistance that resulted from using forced convection condensation in the condenser.

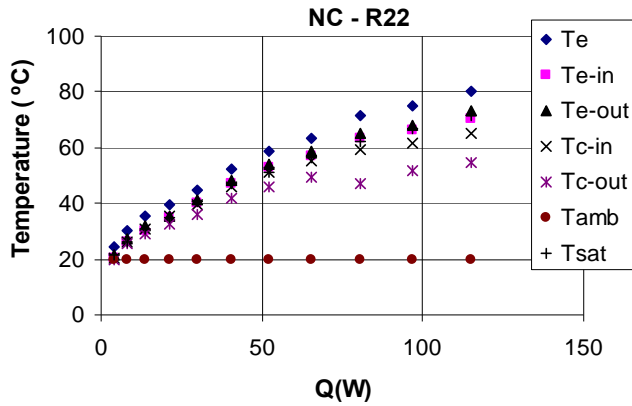**6.3.5 Temperature Distribution in the Thermosyphon System at Different Heat Loads for R22 Using NC Condensation**

Figure 6.22 shows the distribution of the temperatures at different locations of the thermosyphon system using R22 and natural Convection. The experimental data are shown in Tables 5.12.

NC - R22

Figure 6.22: Temperatures distribution at different heat loads for R22 using evaporator-1 and NC.

6.3.6 Temperature Distribution at Different Heat Loads for R22 Using FC Condensation

Figure 6.23 shows the distribution of the temperatures at different locations of the thermosyphon system using R22 and forced Convection. The experimental data are shown in Tables 5.14.

FC - R22
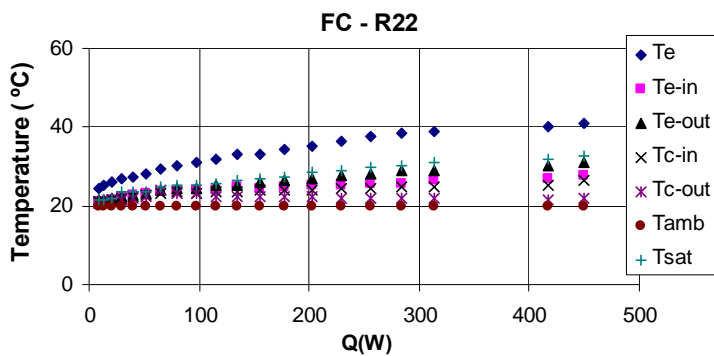
Figure 6.23: Temperatures distribution at different heat loads for R22 using evaporator-1 and FC.

The general behavior of the temperatures distribution in the systems using R22 is similar to high extent to R134a, but with slight difference in the val-

ues of temperatures and corresponding heat load.

R. Khodabandeh, (2004) studied the influence of forced and natural convection cooling of condenser on the temperature distribution at different locations of the thermosyphon loop, using refrigerant Isobutane (R600a) and he found that for natural convection the evaporator temperature reached higher values (55˚C at 60W) than that in forced convection (40˚C at 80W).

Figures 6.24 and 6.25 compares between the behavior of evaporator and the out condenser temperature at different heat loads at both natural and forced convection for R134a and R22, respectively.
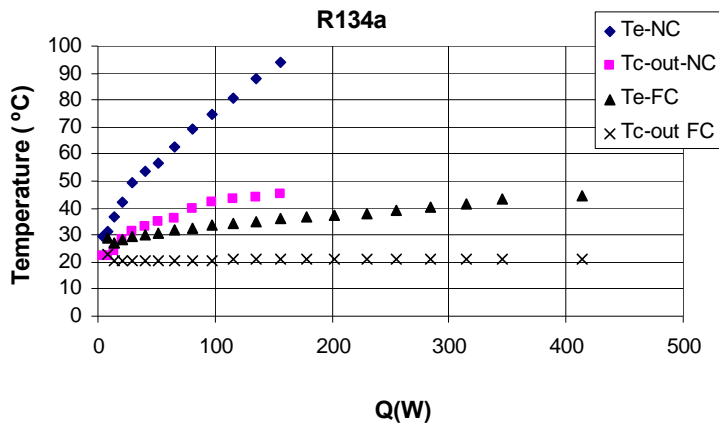
Figure 6.24: Comparison between evaporator temperature at NC and FC using R134a and evaporator-1 at different heat loads.

Both temperatures at natural and forced convection condensation increases linearly with increasing in the heat loads, but with higher slope in the case of natural convection. The maximum evaporator temperature obtained at natural convection is about 94˚C at 155W, while it is about 44˚C at 414W in the case of using forced convection.
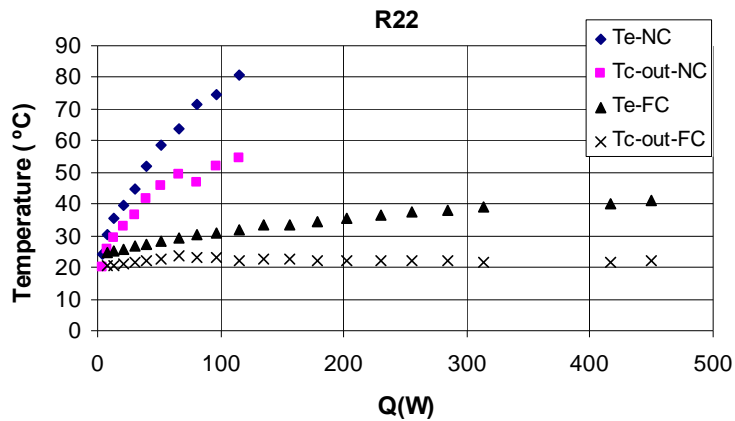
Figure 6.25: Comparison between evaporator temperature at NC and FC using R22 and evaporator-1 at different heat loads.

The same observation is applied in the case of using R22, but with some difference in the obtained values of maximum evaporator temperature and corresponding input heat loads. The maximum evaporator temperature obtained at natural convection is about 80˚C at 115W, while it is about 40˚C at 450W in the case of using forced convection.

Another important observation that should be highlighted from Figures 6.24 and 6.25 is that at natural convection condensation, a higher temperature difference is seen between condenser output and evaporator than forced convection. This is due to efficient condensation in the condenser and low thermal resistance using forced convection.

CHAPTER SEVEN

CONCLUSIONS AND RECOMMENDATIONS

7.1 Conclusions

This section lists the key conclusions of this research. However, detailed conclusions are provided by the end of the main chapters. In light of the furnished analyses and the corresponding discussions, the following are the conclusions:

1. The heat transfer coefficient is highly dependant on the heat applied to the evaporator. It increases approximately linearly with heat applied to the evaporator.

2. The heat transfer coefficient in the thermosyphon system is highly dependant on the type of the refrigerant used, R134a showed better performance than R22.

3. The heat transfer coefficient with free convection condensation is higher than heat transfer coefficient with forced convection condensation at the same heat load and this due to higher saturation pressure in the thermosyphon system at natural convection.

4. The heat flux with free convection condensation mechanism is higher than heat flux with forced convection condensation mechanism at the same heat load and this due to higher saturation pressure in the thermosyphon system at natural convection.

5. The heat flux absorbed in the evaporator channels is proportional to the temperature difference between the evaporator inner surface and the refrigerant saturation temperature, the absorbed heat flux is approximately the same for the two refrigerants used, (R134a and R22) while lower temperature difference observed when R134a is used.

6. The overall heat transfer coefficient (defined in Equation 6.2) in the system for forced convection is higher than for natural convection. This is due to efficient condensation at forced convection, which consequently contributes to low thermal resistance between the condenser and the surrounding. This thermal resistance is greatly depending on the type of convection and the surface area of the condenser.

7. The heat transfer coefficient is highly dependant on the design of evaporator. Two types of evaporators are investigated; the heat transfer coefficient of the evaporator with small heat transfer area was higher than the heat transfer coefficient in the evaporator of high surface area. In other words, the heat transfer coefficient is higher in case of using larger channel diameter.

8. The heat transfer coefficient is direct proportional with the reduced pressure.

9. The temperature difference [$T_{evaporator}$–$T_{saturation}$] is found to be dependent on both the heat flux applied to the evaporator, the pressure inside the system and the type of the refrigerant used.

10. The overall thermal resistance decreased almost linearly with increasing the heat load regardless the type of the refrigerant used. Moreover the thermal resistance is much lower when forced convection heat transfer is applied in the condenser. All of these experimental observation are in line with the theoretical definition of the heat transfer resistance defined in equation (6.4).

11. With natural convection heat load of 150W, the evaporator temperature increased rapidly to about 94˚C with corresponding system pressure

3280kpa. While low and stable temperature of 42˚C is achieved with high heat flux of 420W when forced convection is applied with corresponding system pressure 1000kpa.

—**7.2 Recommendations**

The research encompasses a multitude of parameters at different spatial levels. Several recommendations can be drawn out of this research. The recommendations listed here below support future studies that can address the following issues:

1. A well developed measurement equipments with data acquisition system should be used to monitor the most important parameter in the thermosyphon system such as temperature, pressure and pressure drop.

2. To have efficient cycle in the thermosyphon system, the speed of the fan attached to the condenser should be controlled with respect to the evaporator temperature.

3. The proper weight and pressure of the refrigerant charged in the thermosyphon system is an important parameter for having steady and efficient cycle in the thermosyphon system.

4. The refrigerant charged to the thermosyphon system should be in liquid phase. Other types of refrigerants can be investigated such as R600a and R11.

5. The condenser used in the experiments is horizontally installed as shown in Figure 4.1. This makes some condensation goes back to the riser and consequently decrease the performance of the cycle, so inclining the con-

denser to the side of the down-comer will prevent this phenomenon to happen or at least reduce it.

6. Many other parameters such as the effect of different designs for the evaporator and condenser including the heat transfer area, channels diameter, surface finishing of the channels in addition to the length and diameter of both riser and down comer.

7. The possibility of using transparent pipes instead of traditional copper pipes is very important for monitoring and watching the behavior of the refrigerant inside the thermosyphon system, and thus no need to guess the type of boiling.

References

Ali A.A, (2004**). Design And Analysis of A Compact Two Phase Cooling System For A Laptop Computer**. Msc. thesis in Mechanical Engineering, Georgia Institute of Technology, Georgia, pp. 8

Babic, D., Murray, D. B., Torrance, A. A, (2005). **Mist Jet Cooling of Grinding Processes**, Int. J.Mach. Tools Manufact. 45, pp. 1171-1177.

Bao, Z. Y., D.F. Fletcher, B.S. Haynes, (2000). **"Flow boiling heat transfer of Freon Rll and HCFC123 in narrow passages"**, Int. J. of Heat and Mass Transfer, vol. 43, pp. 3347-3358.

Cengel, Yunus, (2003). **A. Heat Transfer: A Practical Approach**. Second edition. New York, NY: McGraw Hill, pp 785-841.

Chandrashekhar Ramaswamy, Yogendra Joshi, Wataru Nakayama, (1999). **Thermal performance of a compact two-phase thermosyphon: Response to evaporator confinement and transient loads, Enhanced heat transfer**, vol. 6. No. 2-4, pp. 279 – 288.

Cooper, M. G., (1984). **Saturation Nucleate Pool Boiling. A Simple Correlation,** Proc. 1st National Conference on Heat Transfer, Vol. 2, pp. 785-793, (I. Chem. E. Symp. Ser. No. 86).

D. Gorenflo, W. Fath, (1987). **Heat transfer on the outside of finned tubes at high saturation pressures**, in: Proc. XVIIth Internat. Congr. of Refrig., Vienna, Austria, Vol. B, pp. 955–960.

D.S. Steinberg, (1980). **Cooling Techniques for Electronic Equipment**, Wiley, New York.

Faghri, Amin, (1995). **Heat Pipe Science and Technology**. US: Taylor & Francis.

Gorenflo, D., (1993). **Pool Boiling**, in VDI Heat Atlas, VDIVerlag GmbH, Dusseldorf, Germany, pp. Ha1-13.

I. Mudawar, (2000) . **Assessment of high-heat-flux thermal management schemes,** Itherm 2000 Proceedings, vol. 1, Las Vegas, USA, pp. 1–20.

Incropera F.P. and DeWitt D.P, (2002). **Fundamentals of Heat and Mass Transfer**, 5th edition, Wiley.

K.E. Kasza, T. Didascalou, M.W. Wambsganss, in: R.K. Shah (Ed.), (1997). **Microscale flow visualization of nucleate boiling in small channels:** mechanisms influencing heat transfer Proceeding of International conference on compact heat exchanges for the process industries, Begell House, Inc, New York, pp. 343–352.

Klimenko, V.V., (1990). **A generalized correlation for two-phase forced flow heat transfer**, Int. J. Heat Mass Transfer 31 (1990) pp. 541-552.

Lienhard, J. H. and V. K. Dihr, (1973b). **Peak Boiling Heat Flux from Finite Bodies**, Trans. ASME. J. Heat Transfer, Vol. 95, p.152.

M.G. Cooper,(1984). **Heat flow rates in saturated nucleate pool boiling—A wide ranging examination using reduced properties, in: J.P. Hartnett, T.F. Irvine Jr (Eds.), Advances in Heat Transfer**, Vol. 16, Academic Press, Orlando, FL.

Narumanchi, S. V. J., Amon, C. H., Murthy, J. Y., (2003). **Influence of Pulsating Submerged Liquid Jets on Chip-Level Thermal Phenomena**, Transactions of the ASME, Vol. 125, pp. 354-361.

Palm, R. Khodabandeh,(1999). **Choosing working fluid for two-phase thermosyphon systems for cooling of electronics**, proc. Interpack 99, Maui, Hawaii.

P.B.Whalley, (1996). **Two-phase flow and heat transfer**, oxford university Press Inc.,New york ,USA,PP 1-1.

Peterson, G.P., (1994). **An Introduction to Heat Pipes**. Canada : John Wiley & Sons, Inc.

Pioro,I. L., D.C. Groenveld, S. C. Cheng, S. Doerffer, A. Z. Vasic, (2001). **Comparison of CHF measurement in R134a cooled tubes and water CHF look-up table**, Int.J. of Heat and Mass Transfer, vol.44,pp. 73-88.

P. Kew, K. Cornwell, (1997). **Correlations for the prediction of boiling heat transfer in small-diameter channels**, Appl Therm Engng 17 (8–10) 705–715.

R. Khodabandeh, B. Palm, (2002). **Influence of system pressure on the boiling heat transfer coefficient in a closed two-phase thermosyphon loop,** Int. J. Thermal Sci. 41 pp. 619–624, Elsevier.

Rahmatollah Khodabandeh and Bjorn Palm, (2002). **An experimental investigation of influence of the threaded surface on the boiling heat transfer coefficients in vertical narrow channels**, Microscale

Thermophysical Engineering, 6:131-139.

Rahmatollah Khodabandeh, (2005). **Pressure drop in riser and evapora-tor in an advanced two-phase thermosyphon loop**, International Journal of Refrigeration 28 pp. 725-734.

Rahmatollah Khodabandeh, (2004). **Thermal performance of a closed advanced two-phase thermosyphon loop for cooling of radio base stations at different operating conditions**, Applied Thermal Engineering 24 pp. 2643-2655.

R. Khodabandeh, (2005). **Heat transfer in the evaporator of an advanced two-phase thermosyphon loop**, Int. J.Refrigeration, 28 pp. 190-202.

S.H. Rhi, Y. Lee, (1999). **Two-phase loop thermosyphon for cooling of electronic system**, in: G.P. Celata, P. Di Marco, R.K. Shah (Eds.), Two-phase Modeling an Experimentation, pp. 561–568.

Steiner, D. and J. Taborek, (1992). **Flow boiling heat transfer in vertical tubes correlated by an asymptotic model**, Heat Transfer Engineering, vol. 13, pp. 43-69.

Systems Design and Analysis, Inc. (2000). **Spray cooling technologies market investigation**, Indianapolis – USA.

T.W. McDonald, K.S. Hwang, R. Diciccio, (1997). **Thermosyphon loop performance characteristics. Part1-Experimental study**, ASHRAE Trans. 83 (Part II, No. 2467).

Webb, R. L., Gilley, M. D. and Zarnescu, V., (1996). **"Advanced Heat Exchange Technology for Thermoelectric Cooling Devices"**, Pro-

ceedings of the 31st National Heat Transfer Conference, ASME HTD-vol. 329, Vol. 7, pp. 125-133.

Womac, D. J., Aharoni, G., Ramadhyani, S., Incropera, F. P., (1990). **Single Phase Liquid Jet Impingement Cooling of Small Heat Sources,** Proceedings of the International Heat Transfer Conference, pp. 149-154.

جامعة النجاح الوطنية

كلية الدراسات العليا

تبريد الأجهزة الالكترونية ذات التدفق الحراري العالي باستخدام السيفون الحراري ثنائي الطور

إعــــداد

أيســر محــمود مسعــود ياســين

إشـــراف

د.عبــد الرحيــم أبــو صفــا

ب

تبريد الأجهزة الالكترونية ذات التدفق الحراري العالي باستخدام السيفون الحراري ثنائي الطور
إعــــداد
أيســـر محــمود مسعـــود ياســـين
إشــــراف
د.عبـــد الرحيــم أبـــو صفــا

الملـــخـــص

تم بناء نظام تبريد في المختبر للأجهزة الالكترونية ذات التدفق الحراري العالي باستخدام السيفون الحراري ثنائي الطور، حيث تم فحصه تحت ظروف وأوضاع تشغيلية مختلفة .

الدراسة عبارة عن تجارب عملية في المشغل تم من خلالها دراسة معامل الانتقال الحراري، الفرق في درجة الحرارة بين المبخر ووسيط التبريد داخل قنوات المبخر، معامل الانتقال الحراري الكلي، و المقاومة الحرارية الكلية في نظام التبريد. تمت التجارب في ظروف وأوضاع مختلفة؛ حيث تم استخدام ضغوط مختلفة، نوعين مختلفين من وسائط التبريد R134a و R22، تصميمين مختلفين للمبخر، استخدام وسيلة الحَمْل الحراري الحر و الجبري لتحريك الهواء الملامس للمكثف. كمية التدفق الحراري ووسيط التبريد من العوامل التي يتم تغيرها ومعايرتها في النظام .

أُستنتج أن معامل الانتقال الحراري يزداد بعلاقة خطية تقريبية مع الزيادة في الحِمْل الحراري المطبق على المبخر و كذلك مع الزيادة في الضغط، ووجد أيضا انه يعتمد بشكل كبير على نوع وسيلة التبريد حيث أن R134a أبدى فعالية أعلى من R22. معامل الانتقال الحراري اكبر في حالة استخدام طريقة الحَمْل الحراري الحر للتكثيف عنه في حالة استخدام الحَمْل الحراري الجبري لنفس الحِمْل الحراري، بينما وجد أن معامل الانتقال الحراري الكلي في النظام في حالة استخدام وسيلة الحَمْل الحراري الجبري للتكثيف اكبر منه في حالة استخدام الحَمْل الحراري الحر. معامل الانتقال الحراري يعتمد بشكل كبير على تصميم المبخر و بشكل خاص على أقطار القنوات.

وجد أن معامل الانتقال الحراري في حالة استخدام وسيلة الحَمْل الحراري الحر يساوي $27kW/m^2.°C$, $3.7kW/m^2.°C$ باستخدام R134a وR22 على حِمْل حراري $115W$ على الترتيب. بينما وجد أن معامل الانتقال الحراري في حالة استخدام وسيلة الحَمْل الحراري الجبري يساوي $2.4kW/m^2.°C$, $1.6kW/m^2.°C$ باستخدام R134a وR22 , بالترتيب على حِمْل حراري

450W. وجد كذلك أن معامل الانتقال الحراري الكلي في حالة استخدام وسيلة الحَمْل الحراري الجبري يساوي C°.W/m²°9.4k على حِمْل حراري 415W بينما كان C°.W/m²°1.08k على حِمْل حراري 115W في حالة استخدام وسيلة الحَمْل الحراري الحر.

وجد أن الفرق في درجة حرارة المبخر ودرجة حرارة الإشباع لوسيلة التبريد يعتمد على الحِمْل الحراري، الضغط داخل النظام، وكذلك نوع وسيلة التبريد، حيث وجد الفرق في درجة الحرارة في حالة استخدام وسيلة الحَمْل الحراري الحر لا يتجاوز C°1 و يتجاوز C°8 باستخدام R134a وR22, على الترتيب على حِمْل حراري 100W.

درجة حرارة المبخر عند استخدام R134a كانت C°94 على حِمْل حراري 155W و C°44 على حِمْل حراري 414W في حالة استخدام وسيلة الحَمْل الحراري الحر و الجبري، على الترتيب. بينما عند استخدام R22 كانت درجة حرارة المبخر C°80 على حِمْل حراري 115W و C°40 على حِمْل حراري 450W في حالة استخدام وسيلة الحَمْل الحراري الحر و الجبري، على الترتيب.

المقاومة الحرارية الكلية للنظام تنقص بعلاقة خطية إلى حد ما مع الزيادة في الحِمْل الحراري بغض النظر عن نوع وسيلة التبريد المستخدمة. علاوة على ذلك، وجد أن المقاومة الحرارية الكلية اقل بكثير في حالة استخدام وسيلة الحَمْل الحراري الجبري عنه في حالة استخدام وسيلة الحَمْل الحراري الحر للتكثيف.

تم حساب قيمة المقاومة الحرارية الكلية في حالة استخدام وسيلة الحَمْل الحراري الحر للتكثيــف فوجدت تساوي C/W°0.47 على حِمْل حراري 155.6W و C/W°0.53 على حِمْل حراري 115W باستخدام R134a وR22 , بالترتيب. بينما في حالة استخدام وسيلة الحَمْل الحـراري الجبري للتكثيف، وجد ان المقاومة الحرارية الكلية تساوي C/W°0.056 على حِمْـل حـراري 414W و C/W°0.044 على حِمْل حراري 417W باستخدام R134a وR22 , بالترتيــب.

1